Title

Monitoring and Modeling Non-Point Source Contributions of Host-Specific Fecal Contamination in San Pablo Bay

Authors

Wuertz, Stefan
Bombardelli, Fabian A
Sirikanchana, Kwanrawee
et al.

Publication Date

2009-04-23

Monitoring and Modeling Non-Point Source Contributions of Host-Specific Fecal Contamination in San Pablo Bay

Principle Investigators

Stefan Wuertz, Ph.D. and Fabián A. Bombardelli, Ph.D.

(swuertz@ucdavis.edu and fabombardelli@ucdavis.edu)

Department of Civil and Environmental Engineering,
University of California at Davis
One Shields Ave., EU III, Davis, CA 95616

Report Authors

Kwanrawee Sirikanchana, Ph.D.
Fabián A. Bombardelli, Ph.D.
Dan Wang
Stefan Wuertz, Ph.D.

With the collaboration of Kaveh Zamani, Sanjeev Jha, Jeff Tolentino,
Laura Doyle and Sungwoo Bae

UC Water Resources Center
Technical Completion Report Project No. WR1015

December 2008

Table of Contents

Acknowledgements

The authors would like to thank the Cooperative Institute for Coastal and Estuarine Environmental Technology (CICEET) for additional financial support that greatly aided collaborative research efforts and outreach activities. Dr. Drew M. Talley, research coordinator at Romberg Tiburon Center for Environmental Studies (RTC), San Francisco National Environmental Research Reserve (NERR), Tiburon, CA, is acknowledged for his assistance in recommending specific sampling sites and facilitating the use of a research vessel through the San Francisco State University Marine Operations. David Bell, Marine Superintendent/Dive Safety Officer, and David Morgan, a vessel operator, are thankfully acknowledged for their capable assistance in operating the *Questuary*, which was used for water sampling in the bay.

Ms. Marina Psaros, a coastal training program coordinator from the RTC, is acknowledged for her assistance in facilitating the outreach activities of this project, including maintaining a project website hosted at the San Francisco Bay NERR website, and organizing an outreach workshop to introduce the project to potential users of the modeling and receiving direct feedback for the project improvement. These activities were funded by CICEET but included results from our UC Center for Water Resources project. All attendants at our public workshops, including managers, regulators, consultants, engineers, and scientists whose job description involves beach, water resource, and land use management, are gratefully acknowledged for providing useful input into our model development.

The authors would like to specially thank Ms. Tina J. Low, P.E., a water resources control engineer from Regional Water Quality Control Board San Francisco Bay Region, Oakland, CA; and Mr. Ken Poerner, a land steward from Solano Land Trust, Fairfield, CA for providing valuable feedback on the project's potential applicability and challenges. Dr. Peter Smith from USGS is also gratefully acknowledged for providing Si3D code.

Lastly, the following postdoctoral and staff researchers, graduate and undergraduate students at University of California, Davis are thanked for their assistance in experiments and water monitoring: Dr. Alexander Schriewer, Asma Rizvi, Jovana Cupovic, Hoang Trang Le, Hong Ly, Shimin Xiao, David Dickey, Ka Chan, Nhaquyen Bui and Jarming Huang.

Abstract

Fecal contamination from non-point sources in coastal and estuarine water bodies is a problem of increasing concern. Water monitoring alone is sometimes insufficient in providing a clear picture of the fecal contamination of a water body. Well-formulated and developed mathematical and numerical transport models, on the contrary, predict continuous concentrations of microbial indicators under diverse scenarios of interest, and they can quantify fecal source contributions on a land use basis (human versus livestock or wildlife).

The present project has demonstrated the utility of quantitative analyses of fecal contamination in water bodies via new experimental measurement techniques as well as mathematical/numerical modeling of the fate and transport of biological contaminants. San Pablo Bay was selected because there is abundant knowledge about the estuarine system and its tributaries and because of the availability of an existing 3-dimensional model. Environmental monitoring of San Pablo Bay was performed with a Microbial Source Tracking (MST) approach that utilized a validated large-volume (100 L) hollow-fiber ultrafiltration method to concentrate water, which was then tested with quantitative real-time PCR assays to identify and quantify fecal contamination contributed from general and human-, cow- and dog-specific sources. Monitoring of human viral pathogens (adeno- and enteroviruses) was also performed. Additional samples were also collected to enumerate microbial indicators (*E. coli* and enterococci). This was the first time that DNA-based molecular assays, which had been previously validated with fecal samples and wastewater effluents in freshwater studies, were applied to an estuarine environment.

Monitoring results indicated low-level general and human-derived fecal contamination in the bay, while cow- and dog-derived contamination was not detected, except for one sample which contained dog-specific genetic marker. Human viruses were also below the sample detection limit. The pollution was more likely to come from surrounding urban areas or wastewater treatment facilities than from agricultural farm land or wildlife areas. Another application of the study included the validation of quantitative sea bird-specific molecular DNA assays for the purpose of microbial source tracking to enumerate the contribution of sea birds to fecal contamination. The assay was found to possess adequate sensitivity and specificity and could be applied in the future to archived environmental samples to estimate the contribution from sea birds to bacterial fecal loads in San Pablo Bay and its tributaries.

A suite of theoretical and computational tools, ranging from one-dimensional (1-D) to three-dimensional (3-D) models, was developed during this project for the analysis of the fate and transport of *Bacteroidales* gene markers. These models were paired with existing visualization tools. Flow conditions for the sampling dates were simulated and results compared with velocity observations. Exploratory assessments of water quality in the San Pablo Bay allowed for an incipient characterization of the transport conditions in San Pablo Bay. Future work includes the optimization of the water-quality sub-module of the code in order to a) include sediment transport in the bay; b) obtain more reliable results

under a wide set of boundary conditions; and c) be able to simulate a wider set of water-quality parameters. Also, the authors would like to add a user-friendly interface to the code to facilitate decision making by coastal managers.

Introduction and Problem Statement

Coastal water quality is affected by increasing anthropogenic uses. Due to a range of water-related recreational activities, microbial contamination is of particular concern to public health officials. Decision makers are plagued with two major difficulties: (i) determination of the presence, abundance and diversity of pathogens and (ii) identification of the sources of fecal contamination. Historically, the obstacles associated with detecting and enumerating pathogens lead professionals to rely on indicator organisms. Regardless of the preventative measures, severe outbreaks (*Cryptosporidium*: Milwaukee (1993), United Kingdom and Europe; *Escherichia coli* O157:H7: Ontario (2000); Unknown agent: Ireland (1991)) are still prevalent. To prevent future outbreaks, a technique to properly detect and enumerate etiological agents is vital (Straub and Chandler, 2003). Pathogen and indicator concentrations do not correlate well (Smith and Perdek, 2004), and viral pathogens are neither regulated nor properly monitored. Due to these and other issues regarding fecal indicator organisms, U.S. EPA has developed a *Critical Science Plan* and *Criteria Development Plan* to update existing recreation water quality criteria (U.S. EPA, 2007a,b).

Numerous studies of coastal waters have demonstrated the presence of human pathogens and indicator bacteria. In a study of the Florida coastline, 70 to 90 percent of sites tested positive for human enteric viruses (Rose, 2000). In Southern California, over 30 percent of the coastal sites tested had human adenovirus present (Rayl, 2001). Gersberg and colleagues (1995) demonstrated that the opening of the San Elijo Lagoon negatively impacted ocean waters in San Diego. The surf zone sites closest to the mouth of the lagoon did not comply with water-contact standards for pathogens. Jiang and Chu (2004) showed that approximately 50 percent of the urban rivers and creeks in Southern California are contaminated with human adenoviruses. Their research also demonstrated that the majority of the microbial input into the ocean occurred during storm events.

New culture-independent microbial detection methods are being developed targeting the 16S rRNA gene in the order *Bacteroidales* to rapidly identify fecal sources and their association with specific pathogens (Savichtcheva et al., 2007; Walters et al., 2007) in water samples. *Bacteroidales* is an anaerobic bacterial order that is prevalent in warm-blooded animals' gastrointestinal systems. Its use as an animal-specific source indicator for fecal contamination is currently increasing (Bernhard and Field, 2000; Dick and Field, 2004; Seurinck et al., 2005; Reischer et al., 2006; Layton et al., 2006; Kildare et al., 2007; Okabe et al., 2007; Reischer et al., 2007), in light of increasing evidence that traditional fecal indicator bacteria, such as *E. coli* and Enterococci, can survive and replicate in the environment. Microbial source tracking (MST) and pathogen detection using PCR techniques to detect genetic markers for a variety of fecal organisms and pathogens have been applied to distinguish human versus non human fecal pollution in

water samples and identify fecal pathogens at lower concentrations and also more rapidly than is often possible with microscopic and cell culture-based methods (Rajal et al., 2007b). MST provides a more complete picture of the land uses and environmental health risks associated with fecal pollution loading in a watershed than is currently possible with traditional indicators and methods.

San Pablo Bay, a northern sub-embayment of San Francisco Bay, is surrounded by 3 watersheds that exceed pathogen water quality standards identified by the California Environmental Protection Agency. The appropriate control measures cannot take place without identifying the contamination sources, whether through storm water runoff from the Bay's surrounding urban area, farm land, or wild life area. A recent year-long microbial source tracking study carried out by the PI revealed that the majority of fecal indicator counts during storm events in Calleguas Creek Watershed were due to non-human sources (Kildare et al., 2006). In the San Francisco Bay region, microbial contamination of surface waters is a major concern to environmental managers and public health personnel.

Yet, regular monitoring alone is sometimes inadequate in providing a clear picture of the fecal contamination of a water body, in addition to being expensive when pathogens are monitored directly. Sampling of large water bodies in specific (few) locations, and at certain (discontinuous) times, may prove insufficient in capturing contamination events that require public health management decisions. Also, it may make more difficult the identification of sources of fecal contamination. Well-formulated and developed mathematical and numerical transport models, on the contrary, can predict continuous concentrations of pathogens under diverse scenarios of interest, and can significantly facilitate source identification. It is relatively easy and inexpensive (as compared with intensive field campaigns) to change boundary conditions in a numerical model in order to simulate diverse sources of contamination. It is also feasible to introduce new parameters into the numerical model to assess the relevance and importance of a given process. Therefore, this study employed mathematical and numerical transport models in concert with new molecular techniques to (i) characterize the sources of fecal contamination of water bodies and (ii) quantify the loads and distributions of *Bacteroidales* marker DNA sequences originating from different animal hosts in San Pablo Bay.

In this research, the code Si3D was used as a basic engine in our developments. Si3D is a three-dimensional numerical model developed at the United States Geological Survey (USGS) and UC Davis, by Dr. Peter Smith (Smith, 1997; Smith and Larock, 1997). It is currently employed by faculty at UC Davis to study diverse estuarine and riverine systems in northern California. It is used to simulate a portion of the Sacramento River, the Consumnes River floodplain, and the Stockton ship canal. The model has also been used for some time to simulate tidal flow of the San Francisco/San Pablo Bay system. The code provides the velocities, water elevations and salinities in the computational domain as a function of time. Figure 1 shows a snapshot of the 3-D flow in the bay looking towards San Pablo Bay. The colored spheres represent mass-less particles that follow the flow. Figure 2 presents the excursion of particles during Neap and Spring tides in San Pablo Bay.

Objectives

The working hypothesis in this study states that a significant portion of the fecal contamination in the estuarine environment is due to non-human contributions such as (i) bird droppings and (ii) urban and agricultural runoff during storm events. Falsification of the hypothesis would be based on the assumption that *Bacteroidales* can be employed for quantitative microbial source tracking. The following milestones were to be addressed:

Objective 1: Develop sea bird (especially sea gull) – specific molecular PCR assays to quantify their contribution to bacterial fecal loads in San Pablo Bay and its tributaries

Objective 2: Monitor 5 locations in the 3 tributaries for *Bacteroidales* and a suite of pathogens during 4 events reflecting both dry and wet weather conditions

Objective 3: Demonstrate the utility of a combination of theoretical/numerical modeling and innovative molecular PCR assays to determine experimentally and then forecast the extent of fecal contamination of a water body, and for the identification of the sources of that contamination

Objective 4: Initiate the development of quantitative tools that could help stakeholders in making decisions to minimize public health risks in San Pablo Bay, e.g., by best management practices aimed at reducing source-specific contamination determined by *Bacteroidales*-based assays

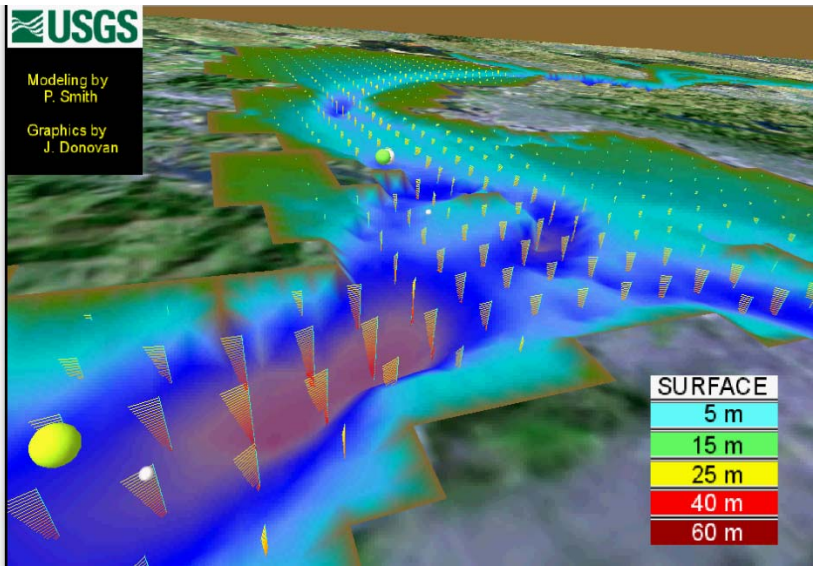

Figure 1. Velocity field obtained with Si3D regarding the tidal flow in San Francisco Bay. The view points to the north to San Pablo Bay from a location close to the Golden Gate; the city of San Francisco is located towards the lower right (Source: USGS website: http://ca.water.usgs.gov/program/sfbay/gr/ptm/index.html.)

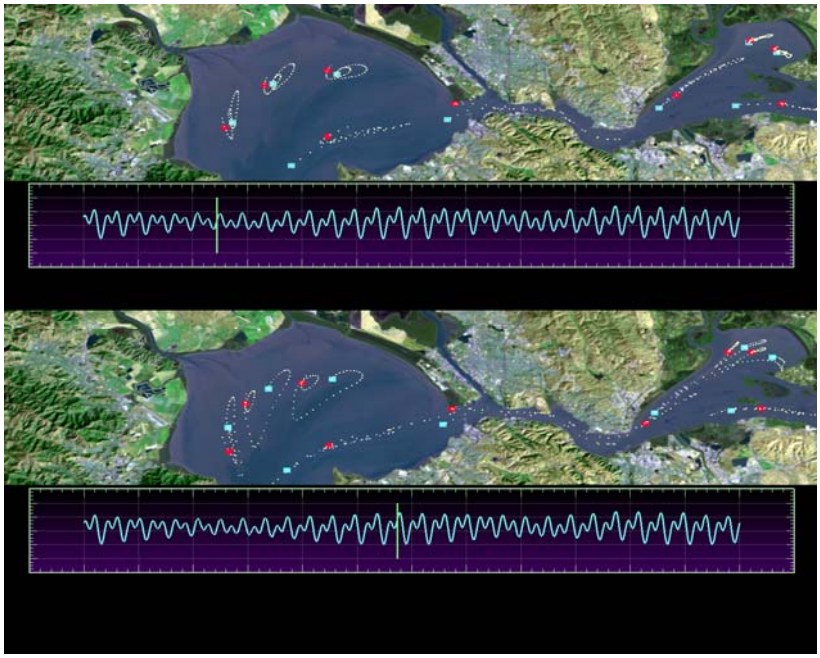

Figure 2. Numerical result obtained with Si3D regarding the trajectories of particles in San Pablo Bay as a function of the tides (Source: USGS website: http://ca.water.usgs.gov/program/sfbay/gr/ptm/index.html.)

Procedure

We approached our research objectives through four major tasks:

Task 1: Development and validation of quantitative sea bird-specific molecular assays for *Bacteroidales* or other suitable target organisms

Task 2: Compilation of field measurements of *Bacteroidales* in San Pablo Bay

Task 3: Mathematical model for the transport of *Bacteroidales* in water bodies and incorporation of a subroutine into the 3-D model Si3D, developed at the USGS; validation of the developed subroutine

Task 4: Application of the resulting numerical model to San Pablo Bay

Task 1: Development and validation of quantitative sea bird-specific molecular assays for Bacteroidales or other suitable target organisms

The original plan of this task was to design real-time TaqMan PCR systems against bird *Bacteroidales* DNA sequences found in the Genbank Database (Pittsburgh Supercomputing Centers, Pittsburgh, PA). Alignment of separate DNA sequences for host-specific *Bacteroidales* isolates has indicated conserved regions suitable bird – specific assays. The designing steps were to follow a similar protocol as for human-specific, dog-specific, and cow-specific assays (Kildare et al., 2007). Specific assays were to be selected based on specific *Bacteroidales* 16S rDNA using Primer Express software (Applied Biosystems, Foster City, CA). All assays were to be validated against a representative number of individual and mixed bird scat samples as well as other wildlife and livestock samples and against a human stool sample collection in the Wuertz laboratory.

Samples from 21 seagull, 3 otter and 5 sea lion stools were received from Melissa A. Miller, Marine Wildlife Veterinary Care and Research Center, Department of Fish and Game in Santa Cruz. All were collected freshly and frozen immediately before transport to UC Davis. We consolidated our previously developed conditional probability analysis based on Bayes' Theorem to calculate probabilities associated with the correct identification of seagull-specific sources when a positive signal is obtained for a particular assay (Kildare et al., 2007). The published primers intended to amplify the whole 16S rRNA, interspace region, and partial 23S rRNA (Dick and Field, 2004) did not amplify any of the 21 fecal samples from gulls. The primers used in another publication by Dr. Field's research group to sequence the *Bacteriodales* 16S rRNA could not amplify any of the 21 samples either (Dick et al., 2005). A different research group reported a similar lack of success in the past (Fogarty and Voytek, 2005). We have found that our own universal *Bacteriodales* qPCR assay BacUni-UCD does amplify *Bacteriodales* in mixed seagull feces (Kildare et al., 2007) albeit fewer gene copies were determined relative to feces from other warm-blooded animals. Significantly, the 21 individual fecal samples listed above could not be amplified with the BacUni-UCD assay. In contrast, 1 out of 3 sea otter fecal samples were amplified as were all 5 sea lion samples.

Due to difficulties encountered when amplifying *Bacteroidales* 16S rRNA genes from seagull feces, we decided to target all bacterial 16S rRNA genes in feces from seagull. Many more animal fecal samples (human, dog, cow, horse, sea otter, sea lion) and sources of guano (pacific loon, common murre, pelican, scaup, scoter, grebe, egret) were obtained from Dr. Michael Ziccardi and his group at the Oiled Wildlife Care Network, UC Davis, and Dr. Woutrina Miller, Veterinary Medicine, UC Davis. The aim was to use DNA extracted from these samples as "subtracter" against seagull guano following the method of subtractive hybridization (Dick and Field, 2004). Bacteria universal primers were used to amplify the entire 16S rRNA region from each fecal sample. Next, the PCR products of the subtracters and seagull fecal samples were digested by AciI endonuclease. The digested DNA pieces from subtracters were ligated to S1 and S2 linkers, while those from seagulls were ligated to T1 and T2 linkers. The ligated DNA from subtracters was then immobilized on a Maxisorp microplate, and the ligated DNA from seagull with

hybridization buffer was added to the plate. Hybridization of DNA originating from seagull guano to subtracter DNA fixed on the plate was carried out under optimized stringency conditions. During this step, the conserved region of seagull guano DNA pieces annealed to the immobilized subtracter fecal DNA, while the unique fragments from seagull remained in solution. This material was then used to try and clone specific 16S rRNA gene fragments associated with seagull feces. Once successfully cloned, the clones were to be screened and sequenced, and seagull-specific primers and a probe were to be designed to target one or more of these unique regions.

While we were busy screening and sequencing clones to identify seagull-specific sequences on the 16S rRNA gene, Lu et al. (2008) published a SYBR Green-based qPCR assay targeting the bacterial species *Catellicoccus marimammalium* in fecal samples from seagulls. Due to the limited amount of time left in the project, we decided to suspend our efforts to develop seagull-specific molecular assays in favor of testing the specificity and sensitivity of the newly published assay. If it could be successfully validated, we would choose to apply the assay to already collected environmental samples and estimate the contribution from sea birds to bacterial fecal loads in San Pablo Bay and its tributaries.

Task 2: Compilation of field measurements of Bacteroidales in the San Pablo Bay

Ten water sampling locations for the environmental monitoring in San Pablo Bay were selected, instead of five as originally planned, after preliminary analysis of mathematical and numerical modeling in San Pablo Bay (see Task 4, Figure 3 and Table 1). Based on the computed velocity vectors at the water surface of the San Pablo Bay, sampling sites were chosen using 4 criteria: 1) locations at the river/creek mouths to measure contaminants in fresh water coming into the Bay from the mouths of Gallinas Creek, Petaluma River, Sonoma Creek, Napa River, and Suisun Bay; 2) locations slightly away from the mouths of freshwater sources to validate the transport model; 3) locations in the bay where there is high enough flow velocity in order to transport the contaminants to the main channel; and 4) locations at the exit channel of water from the Bay towards the middle of San Francisco Bay - the San Pablo Strait. National Oceanic and Atmospheric Administration (NOAA) tidal stations that are nearest to our sampling sites were used as tidal references (Table 2 and Figure 3).

Figure 3. A map of monitoring sites and National Oceanic and Atmospheric Administration (NOAA) tidal stations. Numbers and letters denote individual sites as explained in Tables 1 and 2.

Table 1. Environmental monitoring site names and locations (latitude, longitude)

Site#	Sample	Site name	Latitude, Longitude
1	SPS	San Pablo Strait	+37° 58' 27.03", -122° 26' 20.94"
2	GCCC	Gallinas Creek-China Camp	+38° 0' 44.86", -122° 27' 21.66"
3	GCM	Gallinas Creek Mouth	+38° 0' 31.20", -122° 31' 24.94"
4	PRM[1]	Petaluma River Mouth	+38° 6' 52.79", -122° 30' 21.92"
5	PRMP	Petaluma River-Midshipman Point	+38° 5' 59.87", -122° 27' 0.18"
6	SCM	Sonoma Creek Mouth	+38° 9' 21.64", -122° 24' 23.35"
7	SCINO	Sonoma Creek-Island Number One	+38° 7' 2.41", -122° 22' 56.55"
8	CSMI	Carquinez Strait-Mare Island	+38° 3' 43.73", -122° 15' 47.28"
9	NRMMIS	Napa River Mouth-Mare Island Strait	+38° 7' 1.31", -122° 16' 44.21"
10	CSDP	Carquinez Strait-Dillon Point	+38° 3' 24.63", -122° 11' 41.87"

[1] Location was changed after the first monitoring event from +38° 6' 41.48", -122° 29' 46.31"

Table 2. National Oceanic and Atmospheric Administration (NOAA) tidal station locations used as references to this study's sampling sites

Station#	Station name	Latitude, Longitude	Mean Range (ft)	Spring Range (ft)	Mean Tide Level (ft)
A	Point San Pedro	37° 59.6', -122°26.8'	4.22	5.87	3.16
B	Gallinas, Gallinas Creek	38° 00.9', -122°30.2'	4.3	5.92	3.16
C	Pinole Point	38° 1', -122°22'	4.4	6	3.2
D	Petaluma River Entrance	38° 06.7', -122°29.9'	4.55	6.13	3.28
E	Sonoma Creek	38° 09.4', -122°24.4'	4.21	5.56	2.88
F	Mare Island	38° 04.2', -122°15.0'	4.34	5.86	3.12
G	Vallejo, Mare Island Strait	38° 06.7', -122°16.4'	4.41	5.92	3.15
H	Crockett	38° 03.5', -122°13.4'	4.4	5.94	3.17
I	Benicia	38° 02.6', -122°07.8'	3.93	5.33	2.93

Dr. Drew Talley, a research coordinator from the Romberg Tiburon Center for Environmental Studies, San Francisco National Environmental Research Reserve (NERR) recommended specific sampling sites, which were integrated into the ten sampling locations that had been pinpointed by simulation and modeling as mentioned above. Dr. Talley also facilitated the use of a research vessel suitable for oceanographic research through the San Francisco State University (SFSU) Marine Operations. With the capable assistance of David Bell, Marine Superintendent/Dive Safety Officer, the *Questuary* was used for water sampling in the bay (Figure 4). A few shallow sites were not accessible by boat, and these sites were sampled by car on separate trips.

Figure 4. Photograph of the "Questuary", a research vessel managed by SFSU Marine Operations

Six water sampling events were conducted during the period of November 2007 through July 2008. One-hundred liter samples were collected at each site, except during the first sampling event in November 2007 where 4-L water samples were obtained, to ensure a representative analysis for pathogens that are present at low concentrations in coastal waters. Additional 1-liter samples were collected for total suspended solids (TSS) analysis using Standard Methods 2540D (Eaton et al., 2005). Extra samples were

collected at each site in a sterile container, placed on ice, and shipped back to the UC Davis laboratory within 6 hours of sampling for analysis of traditional fecal indicator bacteria (FIB), *E. coli* and enterococci, using the commercially available kits Colilert-18 and Enterolert (Idexx Inc., Westbrook, Maine). All saltwater samples were 10-fold diluted as recommended by the manufacturer, a necessary step because undiluted water samples gave false positives in both *E. coli* and Enterococci tests. Physicochemical water parameters including pH, temperature, dissolved oxygen, salinity, and conductivity were measured by portable meters. The velocity profile at each sampling site was obtained using the on-board Acoustic Doppler Current Profiler (ADCP), and these data were used to compare model predictions with observations.

After water samples were shipped back to the UC Davis laboratory, hollow fiber ultrafiltration was utilized to reduce the sample to approximately 80 ml using large and small filtration systems (Figure 5). Materials and methods are essentially as outlined by Rajal et al. (2007a,b). The performance of the concentration process was monitored by spiking the sample with the internal standards bacteriophage PP7 and *Acinetobacter* sp. BD413. Recovery efficiency was determined for each sample using the TaqMan quantitative PCR method (Rajal et al., 2007a,b). A QA/QC procedure for volume reduction was developed in a previous project and details are available in Rajal et al. (2005).

Figure 5. Laboratory setups of large (left) and small (right) hollow fiber ultrafiltration systems

The sample retentates after filtration were subjected to DNA extraction and real-time PCR analysis for the detection of *Bacteroidales* markers (universal-, human-, cow-, and dog-specific) and pathogens (adenoviruses and enteroviruses) (Kildare et al., 2007; Rajal et al., 2007b). An additional seagull assay was also used (Lu et al., 2008).

Task 3: Mathematical model for the transport of Bacteroidales in water bodies and incorporation of a subroutine into the 3-D model Si3D, developed at the USGS; validation of the developed subroutine

The mathematical model for transport and fate of *Bacteroidales* in suspension includes the following processes:

a) Time variation in a fixed point;
b) Advection by currents;
c) Diffusion by turbulence;
d) Sources/Sinks.

Within the term Sources/Sinks, it is possible to include processes such as the death rate of *Bacteroidales*, which may include death due to sunlight, described through the half-life of cells; sorption/desorption of *Bacteroidales* to particles, and potential flocculation, by which *Bacteroidales* may form larger particles. If sorption/desorption of *Bacteroidales* to/from particles is found to be important in a given water body, equations representing the concentration of particles in suspension, and the concentration of adsorbed *Bacteroidales* to particles have to be solved. In this case, events of resuspension and deposition of particles on the bay floor need to be analyzed. In mathematical terms, this gives the advection-diffusion-reaction (ADR) equation:

$$\frac{\partial \overline{C}}{\partial t} + \overline{u}\frac{\partial \overline{C}}{\partial x} + \overline{v}\frac{\partial \overline{C}}{\partial y} + \overline{w}\frac{\partial \overline{C}}{\partial z} = \frac{\partial}{\partial x}\left(D_{Txx}\frac{\partial \overline{C}}{\partial x}\right)$$

$$+\frac{\partial}{\partial y}\left(D_{Tyy}\frac{\partial \overline{C}}{\partial y}\right)+\frac{\partial}{\partial z}\left(D_{Tzz}\frac{\partial \overline{C}}{\partial z}\right)-k\overline{C}+Sources/Sinks \qquad (1)$$

where $\overline{C}$ is the local, turbulence averaged *Bacteroidales* concentration; $\overline{u}$, $\overline{v}$ and $\overline{w}$ are the average velocities in the *x*, *y* and *z* directions, respectively; D_{Txx}, D_{Tyy} and D_{Tzz} are the primary components of the effective diffusion tensor; *k* is the decay or mortality rate constant, and *t* is the time coordinate.

Once the mathematical model was defined, several numerical approaches were developed. In a first stage, solutions of the 1-D version of Eq. (1) were developed, in order to obtain useful information such as dispersion coefficients and decay rates from observations in rivers. Then, solutions of the 2-D version of Eq. (1) were developed, in order to address the influence of diverse velocity fields on the transport of *Bacteroidales*. The 1- and 2-D models were validated through comparisons with analytical solutions. Finally, an advection-dispersion-reaction (ADR) equation for *Bacteroidales* in 3-D was considered. The development of the subroutine for *Bacteroidales* and its linking with the basic hydrodynamic code led to Si3D-WQ. All these models and subroutines are developed in FORTRAN and run in a PC.

A comprehensive list of Internet resources was compiled for water quality, flow, and weather data in the San Francisco Bay and Estuary, including the frequencies, periods, and locations in which the data were recorded; these data are crucial for a sound modeling of San Pablo Bay (see McDonald 2007). In addition, we performed a literature review on the modeling of the fate and transport of *Bacteroidales* and other pathogenic indicators (see McDonald 2007).

Task 4: Application of the resulting numerical model to San Pablo Bay

As stated before, the code Si3D serves as the engine for the present project. A word should be devoted herein to explain the reasons for the selection of this code. There are several powerful codes currently being used in the San Francisco Bay in 2- and 3-D modeling: SUNTANS, from Stanford University; UnTRIM, a commercial code originating from the work of Prof. Vincenzo Casulli, from the University of Trento, Italy; Si3D, developed by the USGS; and RMA2, developed at UC Davis in the seventies by Prof. Ian King. The elevated cost of the mature code made UnTRIM unsuitable for the current project; in addition, it is not an open-source code. SUNTANS is based on an unstructured grid which requires a grid generator to operate, and RMA2 is also a commercial code. On the other hand, Si3D is an open-source code which generates its own rectangular grid; it is free of charge; it has a long tradition of simulating the San Francisco Bay; and the developer of the code is readily available in Davis. Because of this feature and because several research groups at UC Davis had been successful in using the code for a number of years, Si3D was selected for this task.

The bathymetry of the San Francisco Bay was obtained from charts available at the USGS. Modeling scenarios representing conditions of interest were selected. These scenarios first included those conditions under which measurements were taken in the bay, as explained in Task 2, i.e., on the days of November 1, 2007; January 15, 2008; March 5, 2008; April 15, 2008; May 28, 2008; and July 9, 2008. This allowed for the comparison of velocities with field data. The boundary conditions for the model are:

a) Stages at the ocean boundary, taken as a weighted value of the stages at Monterey and Point Reyes;
b) Stages at the Sacramento River, taken at stations of Collinsville or Rio Vista;
c) Stages at the San Joaquin River, taken at Antioch.

Convenient scenarios were accommodated to address the issue of the *source* of fecal contamination. Since one of the results of the field campaign was that the sources of contamination did not involve cow- and dog-derived contamination, the scenarios were oriented to potential sources of human contamination. The observation of *Bacteroidales* gene markers during the sampling campaign and exploratory runs allowed for the assessment of the transport conditions of the markers in San Pablo Bay.

Results

Task 1: Development and validation of quantitative sea bird-specific molecular assays for Bacteroidales or other suitable target organisms

We performed qPCR on fecal samples from a variety of sea birds, marine mammals, and terrestrial animals to verify the specificity and sensitivity of the *Catellicoccus marimammalium* 16S rRNA assay (Table 3). Following the method of Lu et al. (2008), 3 ng of total DNA from each fecal extract was tested in 25 μl of qPCR reaction. The assay gave highest sensitivity for fecal extracts from Western gulls. Other extracts were normalized against those of Western gulls at a presumed 100% efficiency of the qPCR reaction. California gulls showed a sensitivity 3 orders of magnitudes lower than that of Western gulls; signals from other sea birds were 1 to 5 orders of magnitude lower; sea otter was 5 orders of magnitude lower; opossum 5 orders of magnitude lower; and dog and horse were 5 orders of magnitude lower. No signals were detected in sea lion, fox, coyote, human and cow fecal samples. The different sensitivities suggest that this assay can detect general fecal pollution stemming from sea birds and that mammals are not or rarely detected. We have tentatively concluded that the assay can be used to estimate the contribution of fecal material from sea birds to San Pablo Bay.

Task 2: Environmental monitoring of Bacteroidales, selected pathogens, and traditional fecal indicator counts in San Pablo Bay

Six environmental monitoring events in San Pablo Bay and its tributaries were carried out during the period of November 2007 through July 2008. The chosen ten sampling sites could not all be accessed by boat due to shallow water near freshwater entries to the Bay. Therefore, water sampling at the Gallinas Creek mouth, Petaluma River mouth, and Sonoma Creek mouth was done by car on a different day. With the separate sampling events, we recorded the weather conditions and any difference in wet and dry conditions of each site was taken into consideration during data analysis.

All but three (event no. 2, sites GCM, PRM, and SCM) samples were collected during dry conditions, where there was no measurable precipitation for at least seven days prior to sampling (Table 4). Fecal indicator bacteria (FIB) concentrations from 10 sampling locations were measured in MPN per 100 mL for *E. coli* and enterococci during events 2 to 6. The FIB counts (*E. coli* and enterococci) for the first monitoring event were not usable because the corresponding IDEXX colorimetric tests were carried out without first making a 10-fold dilution, as recommended by the manufacturer for marine and estuarine samples.

Table 3. Quantitative PCR analysis of fecal samples from a variety of animals using the seagull-specific assay[1] by Lu et al. (2008)

Type of feces/guano	Source of feces/guano	[2]qPCR # of detects/ samples	[3]Gel # of detects/ samples	[4]Ct value		Normalized gene copies (against Western Gull)
				Mean	Standard deviation	
Gull	California Gull	6/6	6/6	25.57	7.22	7.23E-03
	Western Gull	6/6	6/6	18.44	5.9	1
Other Seabirds	Common Murre	1/2	1/2	29.32		5.40E-04
	Pacific Loom	1/1	1/1	23.07		4.07E-02
	White Egret	1/1	1/1	21.57		1.15E-01
	Pelican	2/2	2/2	32.33	0.34	6.74E-05
	Scaup	2/2	2/2	24.4	1.76	1.62E-02
	Scoter	2/2	2/2	19.28	1.27	5.59E-01
	Grebe	2/3	2/3	27.49	5.09	1.92E-03
Marine Mammal	Sea Otter	2/3	2/3	32.77	0.24	4.97E-05
	Sea Lion	1/5	0/5	39.11		6.21E-07
Warm-blooded Animal	Opossum	1/1	1/1	32.8		4.87E-05
	Gray Fox	0/1	0/1			
	Coyote	1/1	0/1	39.24		5.67E-07
	Human Mixed (n=10)	0/1	0/1			
	Cow	2/3	0/3	39.13	0.39	6.12E-07
	Dog	1/3	1/3	31.8	2.02	9.73E-05
	Horse	1/3	1/3	31.93		8.89E-05
	Blank	0/4	0/4	[5]ND	ND	ND

[1] Annealing temperature of 64°C

[2] Number of positive detections per total number of samples tested by quantitative PCR assay

[3] Number of positive detections per total number of samples tested by gel electrophoresis assay

[4] Ct = Quantitative PCR's cycle number when the normalized fluorescense threshold is 0.2

[5]ND = Not detected

Table 4. Water quality parameters and bacterial indicator concentrations of water samples at 10 sampling locations during 6 monitoring events

Event	Site	Date sampled	[1]Weather season	[2]Rainfall condition	DO (mg/L)	pH	T (°C)	Conductivity (S/m) at measured Temperature	Conductivity (S/m) at 25°C	[4]Salinity (part per thousand)	Total suspended solids (mg/L)	*E.coli* (MPN/ 100 mL)	*Enterococci* (MPN/100 mL)
01 (Nov 07)	(1) SPS	1-Nov-07	wet	dry	8.10	7.82	18.2	3.490	NA	27.0	38.31	NA	NA
	(2) GCCC	1-Nov-07	wet	dry	7.64	7.80	16.0	3.410	NA	26.6	37.00	NA	NA
	(3) GCM	NA	NA	NA	NA	NA	NA	NA	NA	NA	NA	NA	NA
	(4) PRM	1-Nov-07	wet	dry	7.10	7.64	16.4	3.160	NA	25.5	181.78	NA	NA
	(5) PRMP	1-Nov-07	wet	dry	NA	7.78	19.1	3.110	NA	24.7	51.44	NA	NA
	(6) SCM	[3]NA	NA	NA	NA	NA	NA	NA	NA	NA	NA	NA	NA
	(7) SCINO	1-Nov-07	wet	dry	8.38	8.05	14.3	3.90	NA	22.7	37.73	NA	NA
	(8) CSMI	1-Nov-07	wet	dry	8.14	7.73	16.5	2.670	NA	20.1	43.39	NA	NA
	(9) NRMM	1-Nov-07	wet	dry	8.18	7.71	18.2	2.550	NA	19.1	36.52	NA	NA
	(10) CSDP	1-Nov-07	wet	dry	8.13	7.75	16.6	2.480	NA	18.5	22.58	NA	NA
02 (Jan 08)	(1) SPS	15-Jan-08	wet	dry	8.46	7.31	9.6	1.710	2.423	14.7	16.70	ND	ND
	(2) GCCC	15-Jan-08	wet	dry	8.10	7.48	9.7	1.756	2.483	15.1	16.20	ND	ND
	(3) GCM	22-Jan-08	wet	wet	7.20	7.27	7.5	1.419	2.127	12.7	71.50	219	156.7
	(4) PRM	22-Jan-08	wet	wet	8.22	7.17	7.9	1.481	2.206	13.2	103.50	ND	ND
	(5) PRMP	15-Jan-08	wet	dry	7.55	7.27	9.8	1.250	1.756	10.4	40.20	ND	ND
	(6) SCM	22-Jan-08	wet	wet	7.45	7.31	7.8	1.516	2.263	13.6	107.70	ND	ND
	(7) SCINO	NA	NA	NA	NA	NA	NA	NA	NA	NA	NA	NA	NA
	(8) CSMI	15-Jan-08	wet	dry	8.42	7.43	9.2	1.471	2.108	1.3	10.00	24.3	ND
	(9) NRMM	15-Jan-08	wet	dry	7.72	6.98	9.3	1.125	NA	9.4	44.40	30.7	11.7
	(10) CSDP	15-Jan-08	wet	dry	7.78	7.42	9.0	1.158	1.600	9.8	25.00	17	ND
03 (Mar 08)	(1) SPS	5-Mar-08	wet	dry	6.63	7.98	12.1	2.364	3.153	19.6	9.20	ND	ND
	(2) GCCC	5-Mar-08	wet	dry	8.24	7.99	12.6	2.456	3.234	20.2	34.93	ND	ND
	(3) GCM	12-Mar-08	wet	dry	7.03	7.55	15.8	0.234	0.283	1.5	49.60	27	13.3
	(4) PRM	12-Mar-08	wet	dry	6.56	7.61	15.1	1.090	1.341	7.8	48.01	25.7	ND
	(5) PRMP	5-Mar-08	wet	dry	8.41	8.16	12.9	1.664	2.165	13.0	14.50	10	ND
	(6) SCM	12-Mar-08	wet	dry	6.44	7.33	15.1	0.696	0.857	4.8	175.00	34.3	23.7
	(7) SCINO	5-Mar-08	wet	dry	7.96	7.90	13.4	1.580	2.025	12.1	17.00	ND	ND
	(8) CSMI	5-Mar-08	wet	dry	8.04	7.43	12.1	1.305	1.737	10.3	12.70	ND	ND
	(9) NRMM	5-Mar-08	wet	dry	7.31	7.76	13.1	1.575	2.038	12.2	25.30	15	ND
	(10) CSDP	5-Mar-08	wet	dry	8.16	7.73	12.2	1.031	1.368	7.9	18.10	11.7	ND
04 (Apr 08)	(1) SPS	15-Apr-08	dry	dry	7.64	8.07	15.3	2.911	3.582	22.6	6.56	ND	ND
	(2) GCCC	15-Apr-08	dry	dry	7.91	8.06	14.4	1.397	1.753	20.4	18.13	ND	ND
	(3) GCM	9-Apr-08	dry	dry	5.10	7.62	14.2	0.557	0.700	3.9	79.12	36.3	48
	(4) PRM	9-Apr-08	dry	dry	6.74	8.02	14.6	1.844	2.301	13.9	52.00	38	ND
	(5) PRMP	15-Apr-08	dry	dry	7.55	8.41	15.2	2.532	3.108	19.3	11.87	11.7	ND
	(6) SCM	NA	NA	NA	NA	NA	NA	NA	NA	NA	NA	NA	NA
	(7) SCINO	15-Apr-08	dry	dry	7.36	8.65	15.2	2.464	3.032	18.8	10.20	ND	ND
	(8) CSMI	15-Apr-08	dry	dry	7.61	8.00	14.8	2.290	2.844	17.6	11.93	ND	ND
	(9) NRMM	15-Apr-08	dry	dry	7.36	7.85	16.1	0.877	1.054	6.0	132.60	11.7	ND
	(10) CSDP	15-Apr-08	dry	dry	9.09	7.90	14.7	1.873	2.332	14.1	14.10	ND	ND

Table 4. (Cont'd) Water quality parameters and bacterial indicator concentrations of water samples at 10 sampling locations during 6 monitoring events

Event	Site	Date sampled	[1]Weather season	[2]Rainfall condition	DO (mg/L)	pH	T (°C)	Conductivity (S/m) at measured Temperature	Conductivity (S/m) at 25°C	[4]Salinity (part per thousand)	Total suspended solids(mg/L)	*E.coli* (MPN/100 mL)	*Enterococci* (MPN/100 mL)
05 (May and June 08)	(1) SPS	28-May-08	dry	dry	8.65	8.08	16.9	2.511	2.978	18.5	8.47	ND	ND
	(2) GCCC	28-May-08	dry	dry	8.81	8.01	16.7	2.828	3.360	21.1	7.89	ND	ND
	(3) GCM	12-Jun-08	dry	dry	6.51	8.02	28.6	4.112	3.856	24.5	73.10	ND	ND
	(4) PRM	12-Jun-08	dry	dry	4.30	7.80	24.8	3.639	3.639	23.0	51.10	ND	ND
	(5) PRMP	28-May-08	dry	dry	7.79	8.33	18.7	3.055	3.475	21.9	39.00	ND	ND
	(6) SCM	12-Jun-08	dry	dry	4.74	7.80	23.8	3.589	3.689	23.2	39.10	20	31
	(7) SCINO	28-May-08	dry	dry	8.22	8.24	17.7	2.911	3.383	21.3	12.64	ND	ND
	(8) CSMI	28-May-08	dry	dry	9.58	7.99	17.2	2.434	2.859	17.7	14.24	ND	ND
	(9) NRMMI	28-May-08	dry	dry	8.83	8.00	16.8	2.073	2.455	15.0	40.40	ND	ND
	(10) CSDP	28-May-08	dry	dry	8.30	7.93	16.7	1.906	2.259	13.7	15.65	ND	ND
06 (July 08)	(1) SPS	9-Jul-08	dry	dry	7.56	7.89	19.7	3.383	3.773	23.9	6.01	ND	ND
	(2) GCCC	9-Jul-08	dry	dry	7.92	7.67	20.5	3.395	3.706	23.6	9.16	ND	ND
	(3) GCM	15-Jul-08	dry	dry	5.54	7.78	25.7	4.028	3.998	25.5	45.90	101.7	22
	(4) PRM	15-Jul-08	dry	dry	6.10	7.83	22.4	3.609	3.798	24.1	42.60	ND	13.3
	(5) PRMP	9-Jul-08	dry	dry	7.52	7.86	23.0	3.536	3.677	23.3	44.50	ND	ND
	(6) SCM	15-Jul-08	dry	dry	6.37	7.91	22.0	3.484	3.687	23.4	104.40	10	ND
	(7) SCINO	9-Jul-08	dry	dry	7.55	7.91	22.0	3.296	3.497	22.0	51.30	ND	ND
	(8) CSMI	9-Jul-08	dry	dry	7.53	7.75	20.2	2.957	3.263	20.4	8.58	ND	ND
	(9) NRMMI	9-Jul-08	dry	dry	8.09	7.76	21.9	2.604	2.767	17.0	39.40	10	ND
	(10) CSDP	9-Jul-08	dry	dry	9.30	7.87	20.4	2.374	2.604	15.9	9.00	ND	ND
Minimum					4.30	6.98	7.50	0.23	0.28	1.26	6.01	ND	ND
Maximum					9.58	8.65	28.60	4.11	4.00	26.95	181.78	219.00	156.70
Median					7.72	7.81	15.90	2.43	2.60	18.48	36.76	22.15	22.85
[5]Geometric mean					8.34	8.56	17.64	2.47	2.92	18.61	44.85	16.75	11.14

[1]Weather seasons: dry = April to October; wet = November to March

[2]Rainfall conditions: dry = defined as having at least seven days without measurable precipitation prior to sampling; wet = defined as conducting after a storm that produces at least 0.5 inches of precipitation after a dry period

[3]NA = not available

[4]ND = not detected. The detection limit was 10 MPN/100 mL

[5]Geometric mean was calculated with 0.5*detection limit for ND data

The detection limit for *E. coli* and enterococci in this study was 10 MPN per 100 mL. Sixty-two percent (30 out of 48 samples) of water samples had *E. coli* nondetects, and 83% (40 out of 48 samples) had enterococci nondetects (Table 4). The median concentrations for *E. coli* and enterococci were 22.15 and 22.85 MPN per 100 mL, respectively, where the maximum concentrations were 219 and 156.7 MPN per 100 mL for *E. coli* and enterococci, respectively. The US EPA bacteriological criteria for water contact recreation in moderately used freshwater areas are 298 and 89 CFU per 100 mL for *E. coli* and for enterococci, respectively, whereas the water quality objective for moderately utilized saltwater is 124 cfu per 100 mL for enterococci (CRWQCB, 2007). Taken together, the bacterial indicator data collected during this study indicate no violation of the criteria, except in one sample for enterococci. Sampling sites that had detectable bacterial indicator concentrations include sites GCM, PRM, SCM, and NRMMIS, all of which are located near the freshwater sources entering San Pablo Bay. The bacterial indicator concentrations from the same site were fairly consistent throughout all 5 sampling events, with the exception of site GCM, which showed peak concentrations for both *E. coli* and enterococci during sampling event 2. Site GCM is located very close to a residential area and had the most variable indicator concentrations.

Higher and more variable concentrations of both *E. coli* and enterococci were detected during the wet season (Figure 6), suggesting that the indicator concentrations from sites adjacent to freshwater sources were influenced by storm runoff from land.

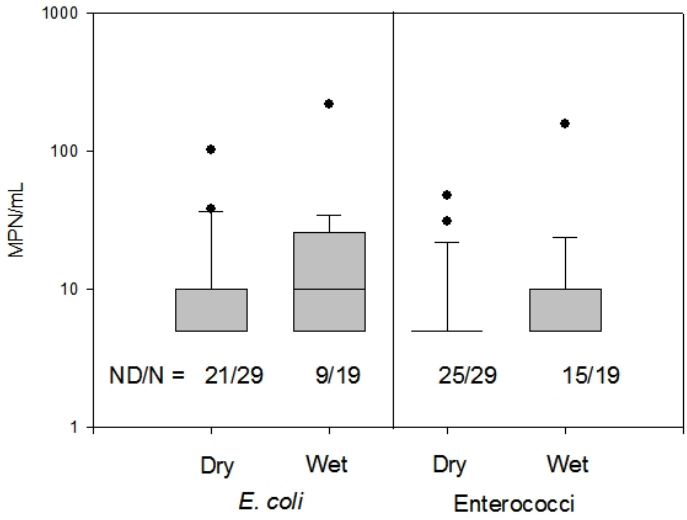

Figure 6. Seasonal concentrations of *E. coli* and enterococci in San Pablo Bay and its tributaries. The boxes span from the estimated 25th to 75th percentile values, with the median in between. The bars with whiskers span from estimated 10th to 90th percentile values, and markers indicate 5th and 95th percentile values. Data points that were nondetects were calculated as 50% of the detection limit, which in this study was 50% * 10 = 5 MPN per 100 mL. Wet season refers to water sampling in January and March 2008, and dry season refers to sampling events in April, May/June, and July 2008. ND = number of nondetects, and N = number of samples

Environmental concentrations of universal *Bacteroidales* were expressed as gene copies per mL of water sample before filtration. Filtration recovery percentage was used as a way to monitor the performance of the concentration process. *Acinetobacter* sp. BD413 was used as the internal standard for *Bacteroidales.* Recovery efficiency was determined for each sample using the TaqMan quantitative PCR method developed in the Wuertz laboratory (Rajal *et al*., 2007a,b). Universal *Bacteroidales* markers were detected in all samples, indicating non host-specific fecal contamination. This 100% positive detection of *Bacteroidales* contrasted with the partial detection of *E. coli* and enterococci during events 2 to 6. Concentrations of universal *Bacteroidales* during events 1 to 6 from November 2007 to July 2008 at all 10 sampling locations ranged from 0.29 to 644 gc/mL (Figure 7). Universal *Bacteroidales* concentrations were higher during the wet season, implying that stormwater runoff increases in universal *Bacteroidales* concentrations in the bay, as expected. The scatter of the data for the wet season is due to the high variability of concentrations in the November 2007 event.

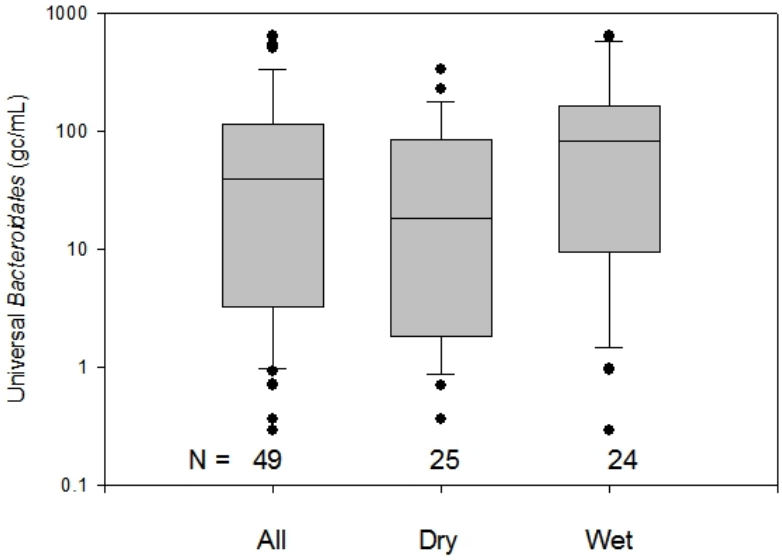

Figure 7. Range of universal *Bacteroidales* concentrations during events 1 to 6 from November 2007 to July 2008 at all 10 sampling locations. Data are presented for the entire period and on a seasonal basis. N = number of samples

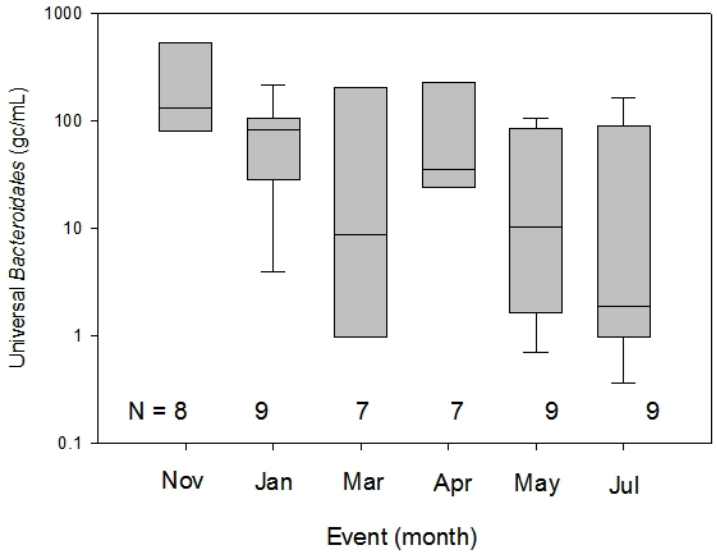

Figure 8. Universal *Bacteroidales* in San Pablo Bay and its tributaries by sampling event

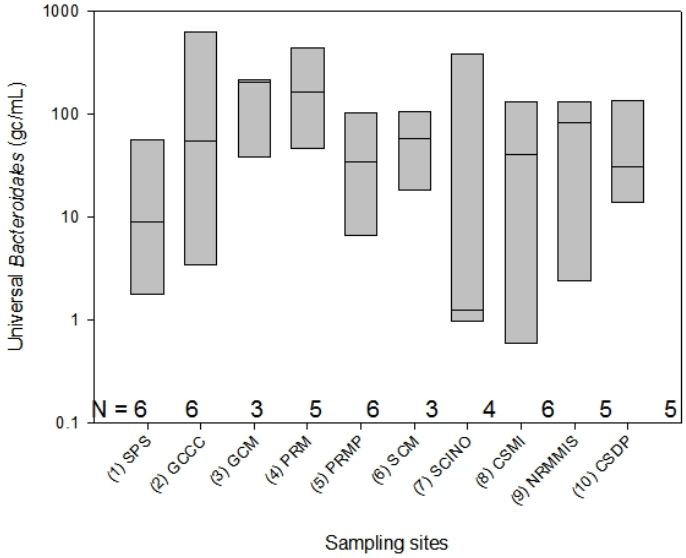

Figure 9. Site-specific patterns of universal *Bacteroidales* in San Pablo Bay and its tributaries

The concentrations at each site varied among events. Highest concentrations of universal *Bacteroidales* were from site 3-GCM, at the Gallinas Creek mouth, located next to a residential area and a storm drain (Figure 9). The lowest concentrations were at site 1-SPS, the San Pablo Strait. There are two possible explanations for the low prevalence of *Bacteroidales* at this site. First, the high flow velocity, due to the existence of the deep channel at this site, can quickly flush out *Bacteroidales* concentrations; second, the concentrations of *Bacteroidales* that were detected at other locations in the bay never

reached site 1-SPS. The modeling of fate and transport of *Bacteroidales* in the bay, as being developed in Tasks 3 and 4, supports this explanation.

Human-specific *Bacteroidales* were detected in 41 out of 55 or 74.5% of samples. The relative amounts of human-specific and universal *Bacteroidales* gene copies were compared (Figure 10). Unlike for universal *Bacteroidales,* there was no seasonal effect. Relative ratios of human-specific to universal *Bacteroidales* concentration were not affected by filtration recovery since the same recovery value for each sample was applied to both species-specific and universal *Bacteroidales*. There was a wide spread of data and several sampling points were extreme outliers. Human-specific to universal *Bacteroidales* ratios ranged from 0.05 to 6.6. These ratios can be used to evaluate the relative impact of human bacteria sources on the overall *Bacteroidales* population. Possible explanations for ratios greater than unity could be that (1) universal *Bacteroidales* markers were detected at lower levels than human *Bacteroidales* markers due to the presence of fewer cells carrying the genetic marker per unit feces than there were cells carrying the human-specific marker, or (2) there were different decay rates in the environment for human-specific and universal *Bacteroidales* markers.

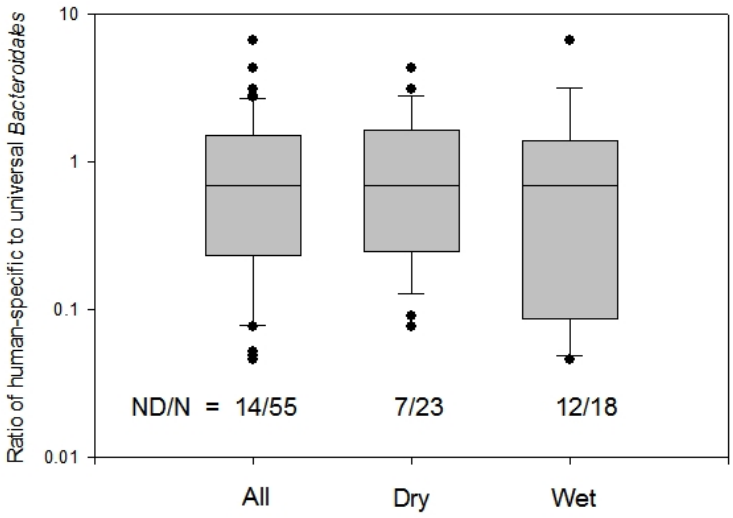

Figure 10. The ratio of human-specific to universal *Bacteroidales* for all water samples during 6 monitoring events. Data are presented for the entire period and on a seasonal basis. ND = number of nondetects, and N = number of total samples.

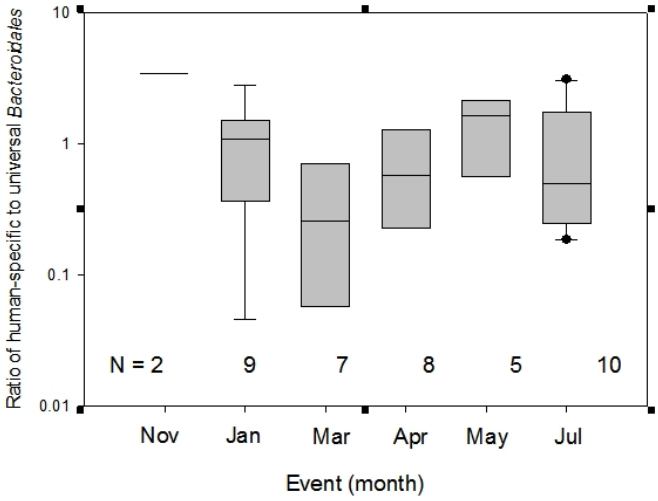

Figure 11. Temporal patterns of ratio of human-specific to universal *Bacteroidales* in San Pablo Bay and its tributaries

Cow- and dog-specific *Bacteroidales* were below detection limits in all samples, except at site GCM during event 2 where the dog genetic marker was detected. It is possible that some fecal contamination of San Pablo Bay may have originated from other sources for which the appropriate host-specific assays have not yet been developed. Field blanks and lab blanks either showed no detects or had levels several magnitudes lower than those of water samples.

Environmental concentrations of selected viral pathogens and their S_{LOD} values were expressed as genomes per ml at each sampling location (Table 5). All major subgroups of human adenoviruses and enteroviruses were assayed for their presence in water samples. No viral pathogens were detected at any sampling location. The average detection limit (S_{LOD}) in all samples was 10 genomes/mL. Filtration recovery was calculated by using spiked bacteriophage PP7 as the internal standard for viruses. S_{LOD} is the sample limit of detection and is determined for all samples, including those that are negative for the pathogens of interest, using the equation developed by Rajal et al. (2007a,b):

$$S_{LOD} = \frac{A_{LOD} \times I \times V_{el} \times V_{RF}}{V_T \times V_{RF,ex} \times V_S \times R_{filtration} \times E_{ex}} \qquad (2)$$

where S_{LOD} (gene copies per ml of original sample) is the sample limit of detection for the target of interest and A_{LOD} (gene copies) is the absolute assay TaqMan detection limit. V is defined as volume in milliliter and represents the following: concentrated retentate (V_{RF}), extracted retentate ($V_{RF,ex}$), nucleic acid extraction eluate (V_{el}), and nucleic acid template added to the PCR reaction (V_T). The volume of the original water sample is V_S. The inhibition factor (I) represents the dilution necessary to produce a positive PCR result and is expressed as the inverse of the dilution factor (ranging from 1 to 500). The overall PP7 recovery, as a fraction, is represented by $R_{filtration}$, while $E_{ex,FLS}$ (0-1) accounts for the nucleic acid extraction efficiency.

Table 5. Environmental concentrations of selected viral pathogens and their sample limit of detection (S_{LOD}) at each sampling location during sampling events 1 to 6

Event	Sample	AdenovirusA, B, C, 40/41		Enterovirus	
		Total Conc in Sample (gc/mL)	S_{LOD} (gc/mL)	Total Conc in Sample (gc/mL)	S_{LOD} (gc/mL)
01 (Nov 07)	(1) SPS	ND	4.77	ND	4.77
	(2) GCCC	ND	12.31	ND	12.31
	(3) GCM	NA	NA	NA	NA
	(4) PRM	ND	9.54	ND	9.54
	(5) PRMP	ND	8.92	ND	8.92
	(6) SCM	NA	NA	NA	NA
	(7) SCINO	ND	61.56	ND	61.56
	(8) CSMI	ND	17.87	ND	17.87
	(9) NRMMIS	ND	2.02	ND	2.02
	(10) CSDP	ND	42.43	ND	42.43
02 (Jan 08)	(1) SPS	ND	0.70	ND	0.70
	(2) GCCC	ND	1.37	ND	1.37
	(3) GCM	ND	0.48	ND	0.48
	(4) PRM	ND	1.27	ND	1.27
	(5) PRMP	ND	29.31	ND	29.31
	(6) SCM	ND	1.05	ND	1.05
	(7) SCINO	NA	NA	NA	NA
	(8) CSMI	ND	4.06	ND	4.06
	(9) NRMMIS	ND	2.93	ND	2.93
	(10) CSDP	ND	0.92	ND	0.92
03 (Mar 08)	(1) SPS	ND	2.90	ND	2.90
	(2) GCCC	ND	11.92	ND	11.92
	(3) GCM	ND	2.04	ND	2.04
	(4) PRM	ND	5.95	ND	5.95
	(5) PRMP	ND	6.07	ND	6.07
	(6) SCM	ND	5.09	ND	5.09
	(7) SCINO	ND	4.69	ND	4.69
	(8) CSMI	ND	0.82	ND	0.82
	(9) NRMMIS	ND	2.16	ND	2.16
	(10) CSDP	ND	4.20	ND	4.20

Table 5. (Cont'd) Environmental concentrations of selected viral pathogens and their sample limit of detection (S_{LOD}) at each sampling location during sampling events 1 to 6

Event	Sample	AdenovirusA, B, C, 40/41		Enterovirus	
		Total Conc in (gc/mL)	S_{LOD} (gc/mL)	Total Conc in (gc/mL)	S_{LOD} (gc/mL)
04 (Apr 08)	(1) SPS	ND	2.88	ND	2.88
	(2) GCCC	ND	30.56	ND	30.56
	(3) GCM	ND	1.64	ND	1.64
	(4) PRM	ND	13.54	ND	13.54
	(5) PRMP	ND	23.66	ND	23.66
	(6) SCM	NA	NA	NA	NA
	(7) SCINO	ND	23.26	ND	23.26
	(8) CSMI	ND	1.37	ND	1.37
	(9) NRMMIS	ND	8.49	ND	8.49
	(10) CSDP	ND	9.57	ND	9.57
05 (May/Jun 08)	(1) SPS	ND	6.00	ND	6.00
	(2) GCCC	ND	0.01	ND	0.01
	(3) GCM	ND	0.92	ND	0.92
	(4) PRM	ND	0.50	ND	0.50
	(5) PRMP	ND	56.37	ND	56.37
	(6) SCM	ND	0.09	ND	0.09
	(7) SCINO	ND	38.65	ND	38.65
	(8) CSMI	ND	45.07	ND	45.07
	(9) NRMMIS	ND	0.19	ND	0.19
	(10) CSDP	ND	69.71	ND	69.71
06 (Jul 08)	(1) SPS	ND	NA	ND	NA
	(2) GCCC	ND	0.00	ND	0.00
	(3) GCM	ND	NA	ND	NA
	(4) PRM	ND	NA	ND	NA
	(5) PRMP	ND	NA	ND	NA
	(6) SCM	ND	0.07	ND	0.07
	(7) SCINO	ND	NA	ND	NA
	(8) CSMI	ND	NA	ND	NA
	(9) NRMMIS	ND	NA	ND	NA
	(10) CSDP	ND	NA	ND	NA

Task 3: Mathematical model for the transport of Bacteroidales in water bodies and incorporation of a subroutine into the 3-D model Si3D, developed at the USGS; validation of the developed subroutine

One-dimensional model

As stated, we developed a 1-D model for the transport and fate of *Bacteroidales* in water bodies, employing several numerical schemes. It is useful to model advection, dispersion, and reactions in one dimension, since the model results can be validated with observations in rivers. Conversely, the model helps to obtain values of the dispersion coefficient and of the decay rates from measurements in rivers. We used finite

differencing to numerically integrate the ADR equation using eight models for advection and three models for dispersion. The eight advection models are:

a) Backward (upwind) differences;
b) Lax dissipative scheme;
c) Lax-Wendroff scheme;
d) leap-frog scheme;
e) fully implicit scheme;
f) McCormack's scheme;
g) Fromm's scheme;
h) and generalized box explicit scheme.

The three dispersion models are: explicit, implicit, and Crank-Nicolson. The finite difference model allows for the simulation of the first-order decay rate of *Bacteroidales*. Each different model was developed in FORTRAN and tested for overall robustness (see McDonald 2007). Any of the advection models may be combined with any of the dispersion models and any of the reaction models to approximate the full ADR equation.

The explicit forms of finite-differencing schemes must satisfy the following stability criteria for advection and dispersion, respectively.

$$u\frac{\Delta t}{\Delta x} < 1 \tag{3}$$

$$D\frac{\Delta t}{\Delta x^2} < \frac{1}{2} \tag{4}$$

The implicit forms of the finite-differencing schemes, however, are stable for all Δx and Δt and, therefore, do not need to satisfy the above stability criteria.

All models sweep once through every spatial position for every forward advancement in time. For explicit models, c_i^{n+1} is solved for each spatial position during each temporal advancement. For implicit models, the coefficients a_i, b_i, c_i and d_i of the equation $a_i c_{i-1}^{n+1} + b_i c_i^{n+1} + c_i c_{i+1}^{n+1} = d_i$ are first found for each spatial position during each temporal advancement; a_1 and c_N are both set equal to zero, and the following tridiagonal matrix is obtained from this system of equations.

$$\begin{bmatrix} b_1 & c_1 & 0 & 0 & 0 \\ a_2 & b_2 & c_2 & 0 & 0 \\ 0 & a_3 & b_3 & \cdot & 0 \\ 0 & 0 & \cdot & \cdot & c_{N-1} \\ 0 & 0 & 0 & a_N & b_N \end{bmatrix} \begin{bmatrix} x_1 \\ x_2 \\ \cdot \\ \cdot \\ x_N \end{bmatrix} = \begin{bmatrix} d_1 \\ d_2 \\ \cdot \\ \cdot \\ d_N \end{bmatrix} \tag{5}$$

The tridiagonal matrix algorithm, also known as the Thomas algorithm, is applied to the coefficients a_i, b_i, c_i and d_i to solve c_i^{n+1} for each spatial position during each temporal advancement.

We have validated all the models by comparing their results with the analytical solutions. Three different problems were devised to test the models. In order to satisfy advection and dispersion stability criteria for all explicit models, the temporal step size was always chosen to satisfy Equations (3) and (4), respectively, for the particular Δx, u and D combination that was being tested.

First, all of the advection models were tested against the advancement of a sharp, unit step front at constant velocity u (Test 1). Its analytical solution is as follows:

$$c = \begin{cases} 1, & x \le ut \\ 0, & x > ut \end{cases} \tag{6}$$

The models were also tested using the Dirac delta function centered at $x = 0$ as the initial condition (Test 2). This condition is explained by Equation (7); however, it must also satisfy the identity in Equation (8).

$$\delta(x) = \begin{cases} \infty, & x = 0 \\ 0, & x \ne 0 \end{cases} \tag{7}$$

$$\int_{-\infty}^{\infty} \delta(x) dx = 1 \tag{8}$$

Applying the advection-dispersion-reaction equation to the Dirac delta function results in the following Gaussian function, which is the analytical solution:

$$c = \frac{e^{-\lambda t - \frac{(x-ut)^2}{4Dt}}}{\sqrt{4\pi Dt}} \tag{9}$$

Test 3 included a case taken from Fletcher (1991), which uses a Neumann boundary condition that varies in time. In this particular case, advection and reactions are not present, meaning that only the dispersion term is needed from the advection-dispersion-reaction (ADR) equation. This equation was solved in the spatial interval $0.1 \le x \le 1$ using the following Neumann boundary condition at $x = 0.1$:

$$\frac{\partial c}{\partial x} = 2 - 2\pi \sin(0.05\pi) \exp\left[-D\left(\frac{\pi}{2}\right)^2 t \right] \tag{10}$$

and a Dirichlet boundary condition of $c = 2$ at $x = 1$.

In Figure 12, we show how the fully implicit scheme performs in advancing the unit step function for Test 1. The undulations and overshooting of the step function illustrate the scheme's inability to accurately model a sharp front. This does not appear to be a problem for smoother fronts or cases where dispersion is important. Figure 13 shows the results of the convergence test for the case of Crank-Nicolson dispersion applied to the Dirac Delta initial condition (Test 2), comparing them with the analytical solution, which is a Gaussian function. Figure 14 shows the results of the convergence test for the case of fully implicit scheme advection with Crank-Nicolson dispersion and a decay rate applied to the Dirac Delta initial condition, again, comparing them with the analytical solution, a Gaussian function. We see from Figures 13 and 14 that fully implicit scheme advection and Crank-Nicolson dispersion both perform very well, even at large space and time steps.

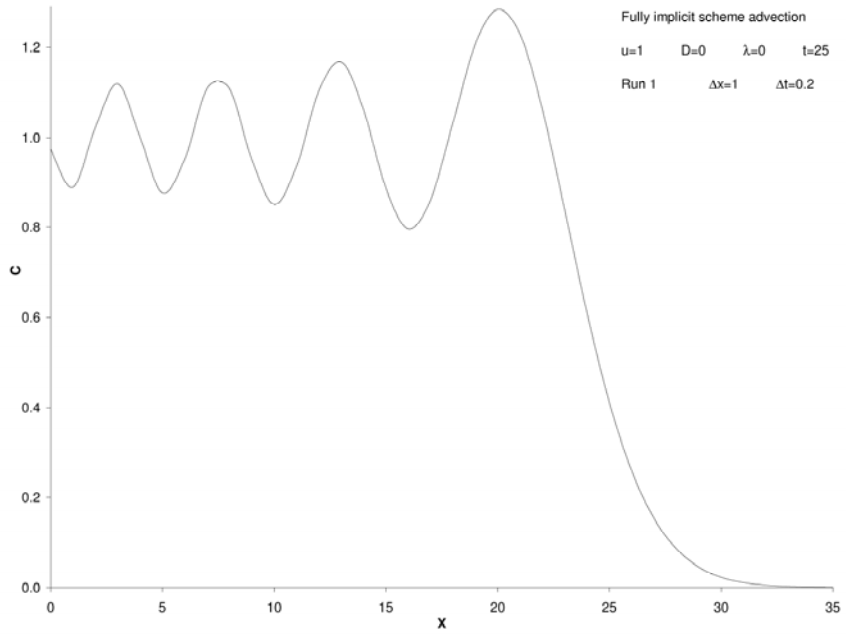

Figure 12. Advection test for the fully implicit scheme applied to the Heaviside function

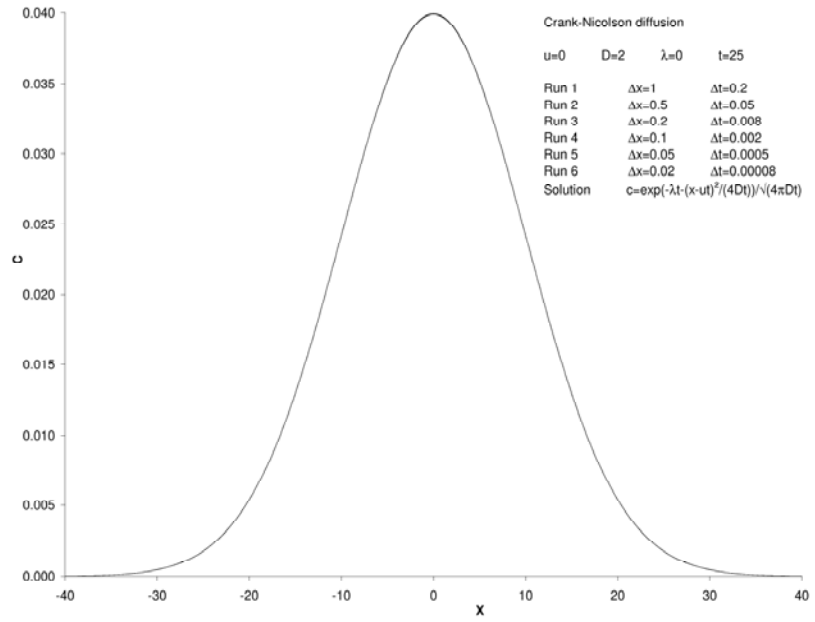

Figure 13. Test for Crank-Nicolson dispersion applied to the Dirac Delta initial condition (Run overlaps with analytical solution)

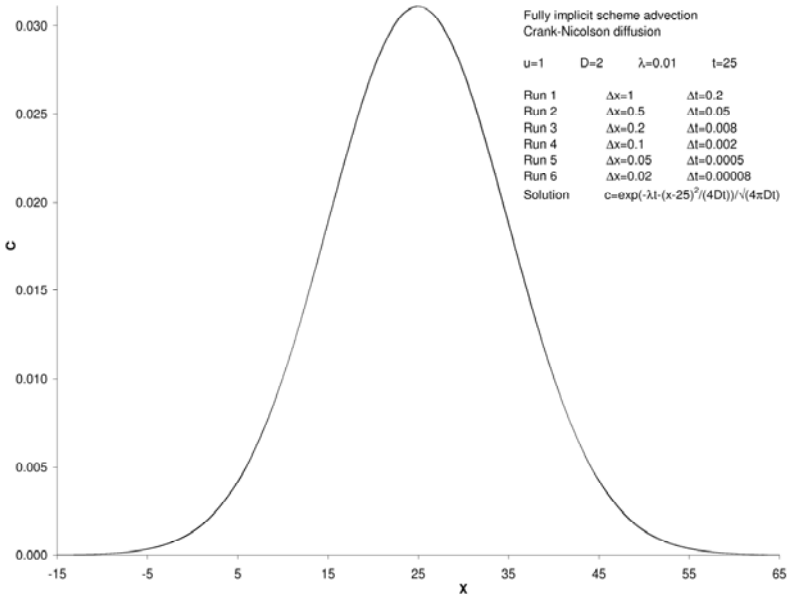

Figure 14. Convergence test for fully implicit scheme advection with Crank-Nicolson dispersion and a decay rate applied to the Dirac Delta initial condition (Runs overlap with analytical solution)

Finally, Figure 15 shows the numerical result for the unsteady dispersion case (Test 3). We can see that the numerical solution overlaps with the analytical counterpart for different times.

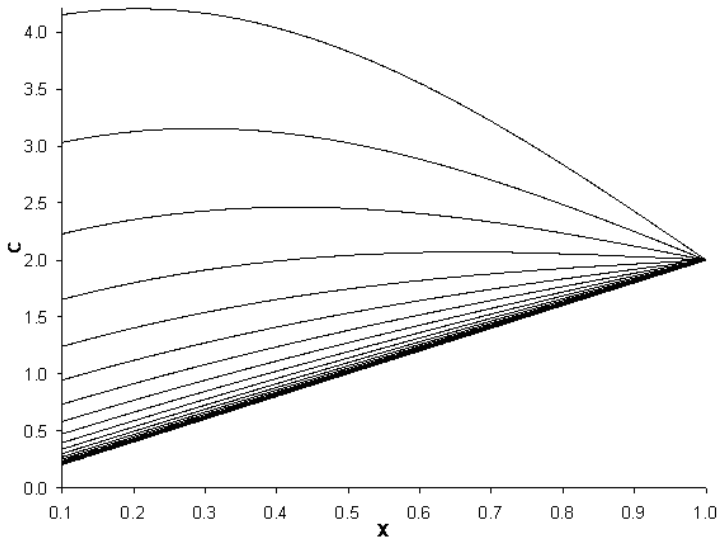

Figure 15: Test results for the Neumann boundary condition case using fully explicit scheme dispersion (modeled results are overlapping the analytical solution)

More details about the numerical implementation of the 1-D models can be found in the MS Thesis of Mr. Anthony McDonald, developed under the supervision of Prof. Bombardelli.

Two-dimensional model

We also developed a 2-D model for the fate and transport of *Bacteroidales* in water bodies. The model solves the ADR equation for a scalar in two dimensions, assuming that the flow velocities are known. We numerically integrated the ADR equation via the finite volume method; the resulting model allows for the simulation of first-order rate decay of *Bacteroidales*. The model has been developed in FORTRAN and runs in a PC. We have validated the model in its different aspects by comparing model results with analytical solutions, and by checking the global correctness of the solutions. We show the set-up for the validation of the numerical solution in an arbitrary rectangle (Figure 16), for which the analytical solution is available (Figure 17). Figure 18 in turn shows contours of concentration of *Bacteroidales* obtained via the numerical solution for the set-up of Figure 16, which compare favorably with the contours of the analytical solution presented in Figure 17. Then, we assessed the behavior of the numerical solution for a case in which we specified a divergence-free velocity field. Figure 19 shows for instance contours of concentration of *Bacteroidales* obtained with our model, superimposed to streamlines of the velocity field. We see that the numerical solution shows expected patterns.

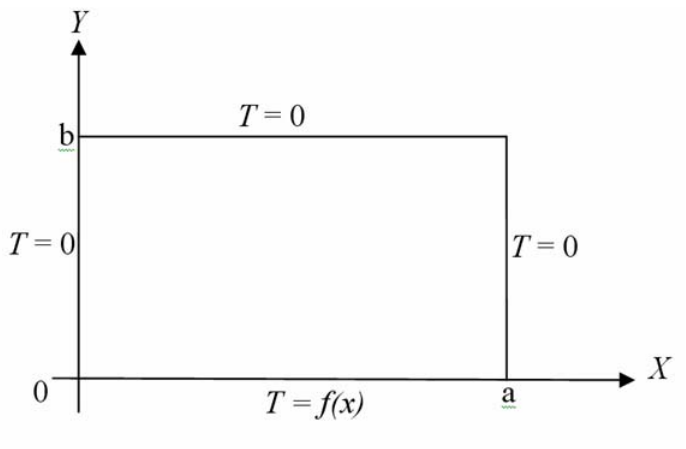

Figure 16. Schematic for the boundary conditions employed to determine the analytical solution of the pure-diffusion equation for *Bacteroidales*. The function specified is a sinusoidal function

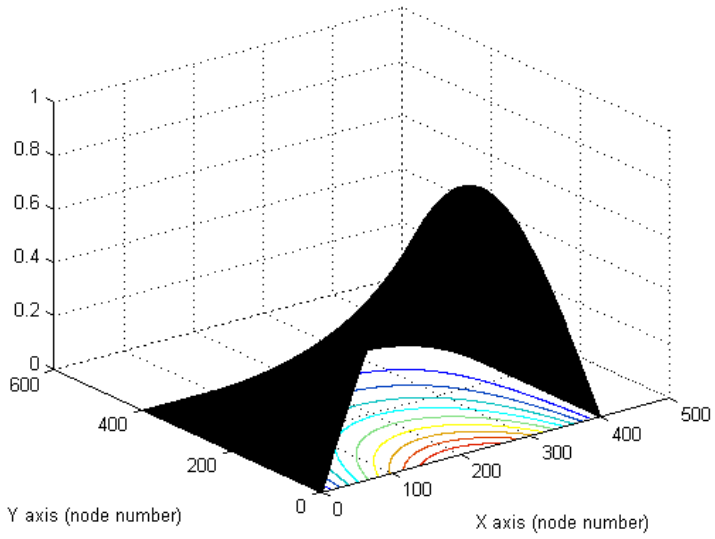

Figure 17. Analytical solution of the diffusion equation of *Bacteroidales* with Dirichlet boundary conditions specified in Figure 16. Contours indicate concentrations of *Bacteroidales.*

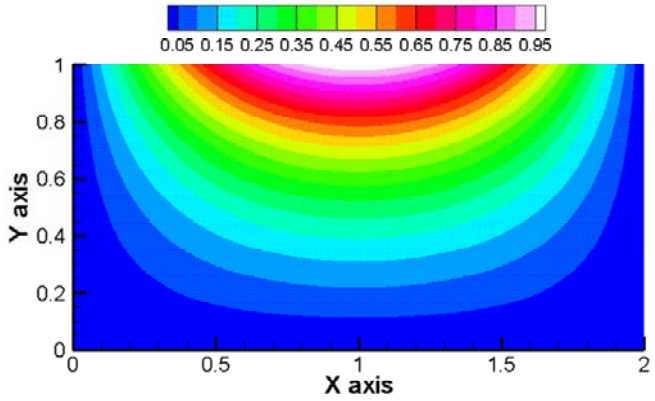

Figure 18. Numerical solution of the diffusion equation of *Bacteroidales* with Dirichlet boundary conditions specified in Figure 16. Contours indicate concentrations of *Bacteroidales*. Two hundred volumes have been used in each direction.

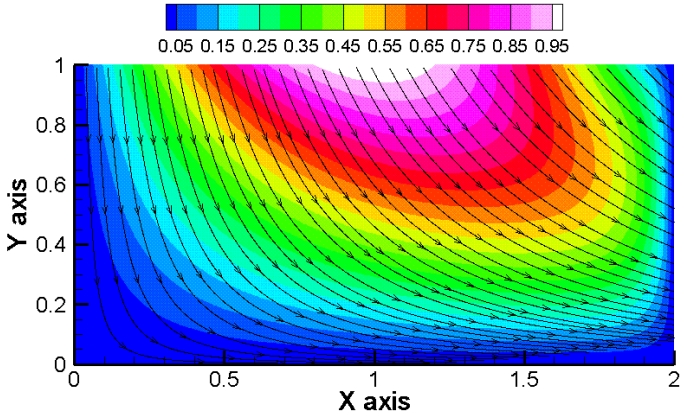

Figure 19. Numerical solutions for the advection-diffusion-reaction equation of *Bacteroidales* with an arbitrary, solenoidal, velocity field, with $A = 1$. Contours indicate concentrations of *Bacteroidales*; streamlines of the steady-state velocity field have also been indicated.

Three-dimensional model

We finished coding the subroutine for transport of *Bacteroidales.* This effort has connections with other projects in our Civil and Environmental Engineering Department at UC Davis in the group of Prof. Schladow (student Mrs. Laura Doyle).

The adopted theoretical model is as follows, which comes from integration of Equation (1) in the layer *k*:

$$\frac{\partial\left(h\,\overline{C}\right)_k}{\partial t}+\frac{\partial\left(u\,h\,\overline{C}\right)_k}{\partial x}+\frac{\partial\left(v\,h\,\overline{C}\right)_k}{\partial y}+\left(w\,\overline{C}\right)\Big|_{k+1/2}^{k-1/2}=\frac{\partial}{\partial x}\left(D_{HB}\;h\,\frac{\partial\overline{C}}{\partial x}\right)_k+$$

$$\frac{\partial}{\partial y}\left(D_{HB}\;h\,\frac{\partial\overline{C}}{\partial y}\right)_k+\left(\frac{J_{zB}}{\rho}\right)\Big|_{k+1/2}^{k-1/2}+Sources/Sinks \qquad (11)$$

where D_{HB} refers to the horizontal eddy diffusivity of *Bacteroidales*, and J_{zB} represents the turbulent vertical flux of *Bacteroidales*. The notation $(\;)\Big|_{k+½}^{k-½}$ represents the difference between interface values for a particular layer. Within the term sources/sinks, processes such as the decay rate of *Bacteroidales* DNA, which may include photoinactivation, are included; sorption/desorption of *Bacteroidales* to particles. The water-quality sub-model, represented by Equation (11) was already implemented in Si3D leading to Si3D-WQ. Although some encouraging exploratory runs have been attempted, more computational work is required herein to have a finalized transport model.

Task 4: Application of the resulting numerical model to San Pablo Bay

Features of the code Si3D

P. E. Smith (1997) authored a semi-implicit, three-dimensional, finite-difference model for estuarine circulation in the FORTRAN 90 programming language. This program was implemented to simulate circulation in the San Francisco Bay and Estuary from the ocean to the Sacramento-San Joaquin Delta. The Si3D program simulates estuarine flows within a 3-D grid which is horizontally resolved by squares and vertically resolved by layers. A bathymetry file identifies which cells are open to flows and which ones are closed. A salinity initial condition is needed, and boundary files are used to indicate water surface elevation, flow rate and salinity, if necessary, for every time increment at each open boundary at the model perimeter. All modeling parameters and output specifications are given in the general input file.

The shallow-water flows of an estuary can essentially be considered horizontal and, therefore, vertical velocities and accelerations are negligible compared to gravity. As a result of this assumption, only the pressure and gravity terms are retained in the *z*-momentum equation, reducing it to the hydrostatic pressure equation. The Coriolis terms in the horizontal momentum equations involving vertical velocity *w* can also be neglected. By incorporating these assumptions, the continuity, *x*-momentum, *y*-momentum, *z*-momentum and salt transport equations become the following five equations, respectively:

$$\frac{\partial u}{\partial x}+\frac{\partial v}{\partial y}+\frac{\partial w}{\partial z}=0 \qquad (12)$$

$$\frac{\partial u}{\partial t}+\frac{\partial uu}{\partial x}+\frac{\partial uv}{\partial y}+\frac{\partial uw}{\partial z}-fv=-\frac{1}{\rho_0}\frac{\partial p}{\partial x}+\frac{\partial}{\partial x}\left(A_H\frac{\partial u}{\partial x}\right)+\frac{\partial}{\partial y}\left(A_H\frac{\partial u}{\partial y}\right)+\frac{\partial}{\partial z}\left(A_V\frac{\partial u}{\partial z}\right) \tag{13}$$

$$\frac{\partial v}{\partial t}+\frac{\partial uv}{\partial x}+\frac{\partial vv}{\partial y}+\frac{\partial vw}{\partial z}+fu=-\frac{1}{\rho_0}\frac{\partial p}{\partial y}+\frac{\partial}{\partial x}\left(A_H\frac{\partial v}{\partial x}\right)+\frac{\partial}{\partial y}\left(A_H\frac{\partial v}{\partial y}\right)+\frac{\partial}{\partial z}\left(A_V\frac{\partial v}{\partial z}\right) \tag{14}$$

$$0=-\frac{1}{\rho_0}\frac{\partial p}{\partial z}-\frac{\rho}{\rho_0}g \tag{15}$$

$$\frac{\partial s}{\partial t}+\frac{\partial us}{\partial x}+\frac{\partial vs}{\partial y}+\frac{\partial ws}{\partial z}=\frac{\partial}{\partial x}\left(D_H\frac{\partial s}{\partial x}\right)+\frac{\partial}{\partial y}\left(D_H\frac{\partial s}{\partial y}\right)+\frac{\partial}{\partial z}\left(D_V\frac{\partial s}{\partial z}\right) \tag{16}$$

where u, v and w are the turbulence-averaged velocities in the x, y and z directions, respectively, and f is the Coriolis parameter. The advective acceleration terms, namely, $\partial uu/\partial x$, $\partial uv/\partial y$, $\partial uw/\partial z$, $\partial uv/\partial x$, $\partial vv/\partial y$, and $\partial vw/\partial z$, are written in a conservative or divergence form. By substituting in baroclinic terms for the pressure gradient terms in the x- and y-momentum equations, assuming $\rho_s = \rho_0$ to the same order of approximation as the Boussinesq approximation, we obtain a form that applies to estuarine tidal flows influenced by density variations.

$$\frac{\partial u}{\partial t}+\frac{\partial uu}{\partial x}+\frac{\partial uv}{\partial y}+\frac{\partial uw}{\partial z}-fv=$$

$$-g\frac{\partial \zeta}{\partial x}-g\frac{1}{\rho_0}\int_z^{\zeta}\frac{\partial \rho}{\partial x}dz'+\frac{\partial}{\partial x}\left(A_H\frac{\partial u}{\partial x}\right)+\frac{\partial}{\partial y}\left(A_H\frac{\partial u}{\partial y}\right)+\frac{\partial}{\partial z}\left(A_V\frac{\partial u}{\partial z}\right) \tag{17}$$

$$\frac{\partial v}{\partial t}+\frac{\partial uv}{\partial x}+\frac{\partial vv}{\partial y}+\frac{\partial vw}{\partial z}+fu=$$

$$-g\frac{\partial \zeta}{\partial y}-g\frac{1}{\rho_0}\int_z^{\zeta}\frac{\partial \rho}{\partial y}dz'+\frac{\partial}{\partial x}\left(A_H\frac{\partial v}{\partial x}\right)+\frac{\partial}{\partial y}\left(A_H\frac{\partial v}{\partial y}\right)+\frac{\partial}{\partial z}\left(A_V\frac{\partial v}{\partial z}\right) \tag{18}$$

The layer-averaged form of the Si3D governing equations is as follows:

Continuity equations:

$$\frac{\partial \zeta}{\partial t}+\frac{\partial}{\partial x}\left(\sum_{k=1}^{km}U_k\right)+\frac{\partial}{\partial y}\left(\sum_{k=1}^{km}V_k\right)=0 \tag{19}$$

$$(w)_{k+½}^{k-½}=-\frac{\partial U_k}{\partial x}-\frac{\partial V_k}{\partial y},\quad k=2,3,\ldots,km \tag{20}$$

Momentum equations:

$$\frac{\partial U_k}{\partial t}+\frac{\partial (Uu)_k}{\partial x}+\frac{\partial (Vu)_k}{\partial y}+(uw)_{k+½}^{k-½}-fV_k+\frac{h_k}{\rho_k}g\rho_1\frac{\partial \zeta}{\partial x}= \tag{21}$$

$$-\frac{h_k}{\rho_k}\left[\frac{gh_1}{2}\frac{\partial \rho_1}{\partial x}+\sum_{m=2}^{k}\left(\frac{gh_{m-1}}{2}\frac{\partial \rho_{m-1}}{\partial x}+\frac{gh_m}{2}\frac{\partial \rho_m}{\partial x}\right)\right]+\frac{\partial}{\partial x}\left(A_H h\frac{\partial u}{\partial x}\right)_k+\frac{\partial}{\partial y}\left(A_H h\frac{\partial u}{\partial y}\right)_k+\left(\frac{\tau_{xz}}{\rho}\right)_{k+½}^{k-½}$$

$$\frac{\partial V_k}{\partial t}+\frac{\partial (Uv)_k}{\partial x}+\frac{\partial (Vv)_k}{\partial y}+(vw)_{k+½}^{k-½}+fU_k+\frac{h_k}{\rho_k}g\rho_1\frac{\partial \zeta}{\partial y}= \tag{22}$$

$$-\frac{h_k}{\rho_k}\left[\frac{gh_1}{2}\frac{\partial\rho_1}{\partial y}+\sum_{m=2}^{k}\left(\frac{gh_{m-1}}{2}\frac{\partial\rho_{m-1}}{\partial y}+\frac{gh_m}{2}\frac{\partial\rho_m}{\partial y}\right)\right]+\frac{\partial}{\partial x}\left(A_H h\frac{\partial v}{\partial x}\right)_k+\frac{\partial}{\partial y}\left(A_H h\frac{\partial v}{\partial y}\right)_k+\left(\frac{\tau_{yz}}{\rho}\right)\Bigg|_{k+½}^{k-½}$$

Salt transport equation:

$$\frac{\partial(hs)_k}{\partial t}+\frac{\partial(uhs)_k}{\partial x}+\frac{\partial(vhs)_k}{\partial y}+(ws)\Big|_{k+½}^{k-½}=\frac{\partial}{\partial x}\left(D_H h\frac{\partial s}{\partial x}\right)_k+\frac{\partial}{\partial y}\left(D_H h\frac{\partial s}{\partial y}\right)_k+\left(\frac{J_z}{\rho}\right)\Bigg|_{k+½}^{k-½} \qquad (23)$$

The notation $(\ )\Big|_{k+½}^{k-½}$ represents the difference between interface values for a particular layer, as before. The layer-averaged density ρ_k has been substituted for ρ_0 in the denominator of the pressure, vertical stress and vertical salt flux terms. This substitution reduces any error caused by the Boussinesq approximation. The bottom and free surface boundary conditions are satisfied by defining $w_{km+½} = 0$, $(uw)_{½} = (uw)_{km+½} = 0$, $(vw)_{½} = (vw)_{km+½} = 0$, $(\tau_{xz},\ \tau_{yz})_{½} = (\tau_{xs},\ \tau_{ys})$, $(\tau_{xz},\ \tau_{yz})_{km+½} = (\tau_{xb},\ \tau_{yb})$, $(ws)_{½} = (ws)_{km+½} = 0$ and $(J_z)_{½} = (J_z)_{km+½} = 0$. The summation term in Equations (19) and (20) is omitted for a surface layer ($k = 1$). These five 3-D governing equations are discretized using semi-implicit leapfrog and semi-implicit trapezoidal finite-differencing schemes (Smith 1997).

To specify the bathymetry for the Si3D code, we retrieved 30-meter digital data from the National Ocean Service's Estuarine Bathymetry (http://estuarinebathymetry.noaa.gov/), a division of the NOAA (National Oceanic and Atmospheric Administration). Figure 20 shows a map of the Si3D modeling area (Source: USGS), and Figure 21 shows a colored contour map of the San Francisco Bay bathymetry developed at UC Davis for this project, based upon the digital elevation model from the NOS. Bathymetric rendering for other resolutions can be found in McDonald (2007).

Previous runs of Si3D have been developed with spatial grids of 500 and 1,000 meters at the USGS. One of the goals of this project is to explore these larger resolutions in the near future, to corroborate the mesh convergence of the solution on salinities, a task rarely developed in estuarine computations. (It is a well-known fact that all numerical solutions need to undergo a rigorous set of tests of mesh convergence in order to guarantee that the numerical results do not depend on the mesh size.)

We decided to focus on modeling the entire bay, as opposed to our original idea of modeling solely the San Pablo Bay. Figure 22 shows the boundary conditions of the model in the Sacramento-San Joaquin River Delta (Source: USGS). Notice that the model boundary on the Sacramento River lies between the stations of Collinsville and Rio Vista and that it is closer to the former; for the San Joaquin River, the boundary is almost coincident with the station of Antioch. Thus, these three stations were used as river boundary conditions for the model.

Previous validation and calibration of the code Si3D

The Si3D code was extensively validated through comparison with analytical solutions, as reported in Smith (1997) and Smith and Larock (1997).

Figure 23 in turn shows a previous result of the Si3D model where it was used to simulate Delta outflow (Source: USGS). The agreement with the observations is very satisfactory with the exception of the main flow peak where the differences are of the order of 15%.

Definition of scenarios for the hydrodynamics and fate and transport of *Bacteroidales*

We started with the scenario of December 1, 1997 for our runs (in agreement with the scenario used by P. E. Smith in Figure 23), and then moved to the scenarios pertaining to the sampling campaign. The first scenario allowed for the definition of the sampling stations presented in Figure 3. Based on our created index of Internet data sources for water quality, flow, and weather data for the San Francisco Bay (McDonald 2007), we were able to obtain data for the boundary conditions of the model.

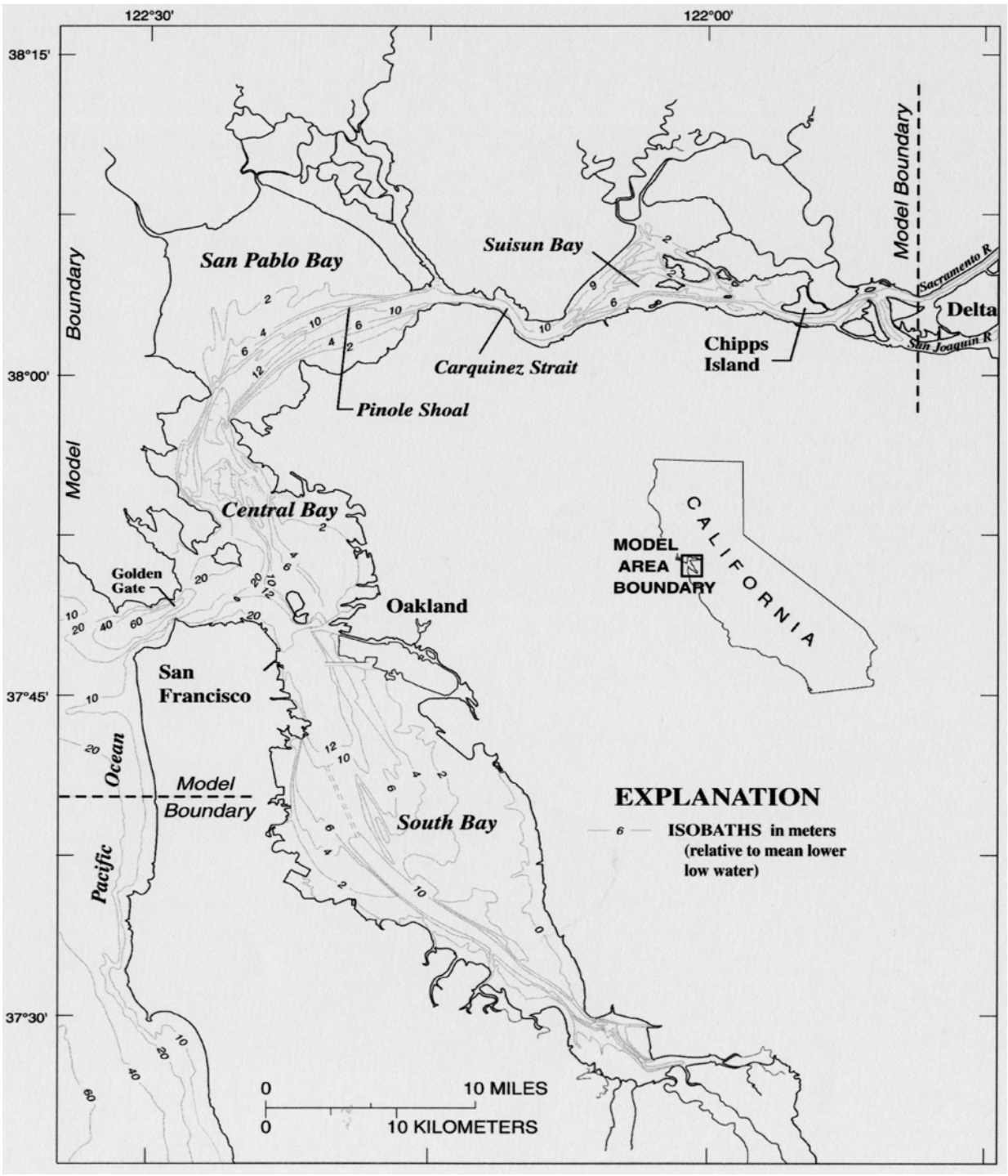

Figure 20. Map of the Si3D modeling area (Source: USGS)

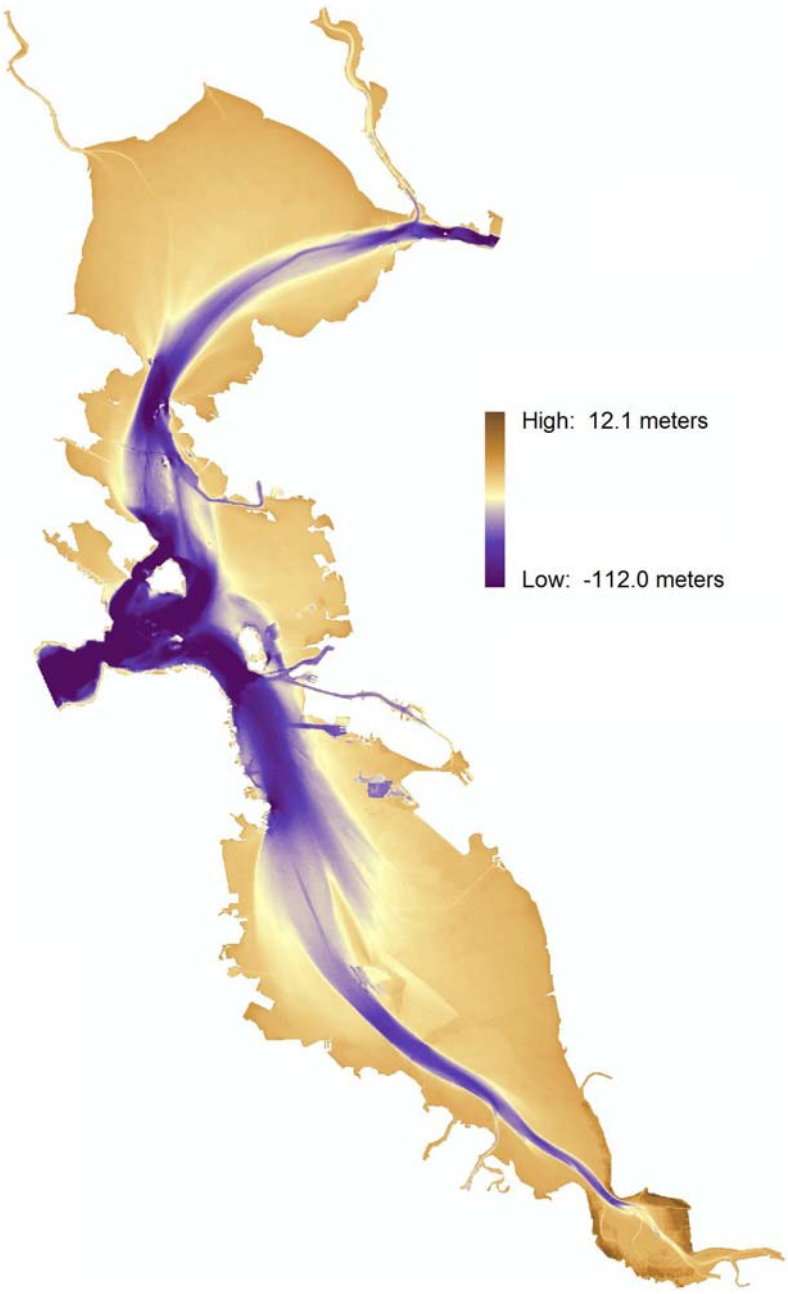

Figure 21. Colored contour map of the San Francisco Bay bathymetry, based upon the 30-meter digital elevation model provided by the National Ocean Service's Estuarine Bathymetry division (http://estuarinebathymetry.noaa.gov/)

Figure 24 shows the grid for the 1,000-m spatial size. The grid is composed by 77 cells in the *x*-axis and by 85 cells in the *y*-axis. The number of cells in the vertical direction is variable, depending on the depth in the bay.

The characteristics of the stage stations for the boundary conditions are as follows:

1) Rio Vista
   Code: RVB
   Maintained by: California Department of Water Resources
   Lat.: 38.15° N; Long.: 121.7° W
   Datum: NAVD
   Conversion distance: NGVD=NAVD-0.742 m
2) Antioch
   Code: ANH
   Maintained by: California Department of Water Resources
   Lat.: 38.018° N; Long.: 121.802° W
   Datum: NAVD
   Conversion distance: NGVD=NAVD-0.741 m

3) Monterey
   Code: 9413450
   Maintained by: NOAA
   Datum: MLLW
   Conversion distance: NGVD=MLLW-0.866 m

4) Point Reyes
   Code: 9415020
   Maintained by: NOAA
   Datum: MLLW
   Conversion distance: NGVD=MLLW-0.805 m

5) Collinsville
   Code: CLL
   Maintained by: California Department of Water Resources
   Lat.: 38.0830° N; Long.: 121.8330° W

The reference level for Si3D in the boundary conditions is NGVD. Data were converted from the original units (ft) to meters, which are the units of Si3D and incorporated in the model. Figure 25 shows the water levels at the boundaries of the domain. For the Sacramento River, the station selected was Collinsville, which was delayed 7 minutes to account for the distance between this station and the location of the boundary condition. When the station selected is Rio Vista, the water levels are moved ahead in time in an estimated 30 minutes interval. The typical two-peak daily variation is seen in Figure 25.

RESULTS FOR DECEMBER 1997

Figures 26 to 29 show numerical results of the flow in San Francisco Bay regarding the distribution of velocity vectors in the surface of the bay for different times. The velocity field information for the free surface can be found in the flow data output file of Si3D, and with a simple algorithm one can isolate and plot the data for the velocity

vectors at the top layer. One such algorithm was implemented in MATLAB at the University of California, Davis, by Mrs. Laura Doyle. The figures show the free surface velocity field during times when the main section of the San Francisco Bay is at high weak tide (hour 13), ebb tide (hour 16), low weak tide (hour 20) and flood tide (hour 23), respectively. Vectors showing the horizontal velocity are plotted at each cell location, and the *x*- and *y*-direction cell numbers are displayed along the edges of these figures.

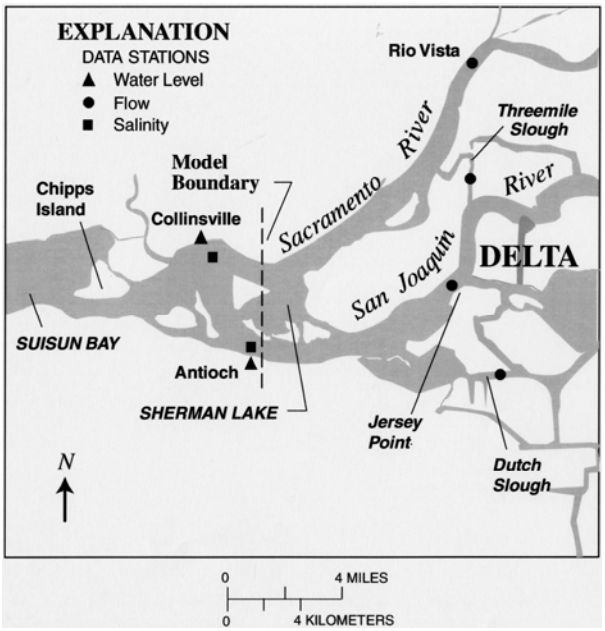

Figure 22. Boundary conditions for the Si3D model in the Sacramento-San Joaquin River Delta (Source: USGS)

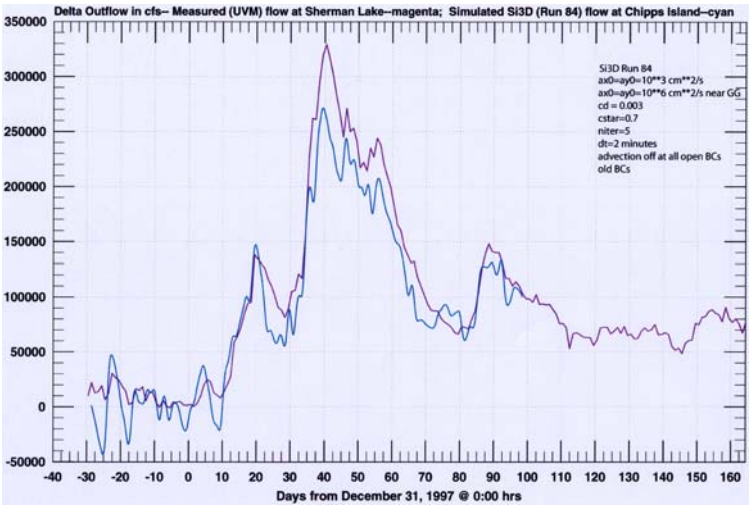

Figure 23. Simulation of delta outflow in Si3D compared with observations (Source: USGS)

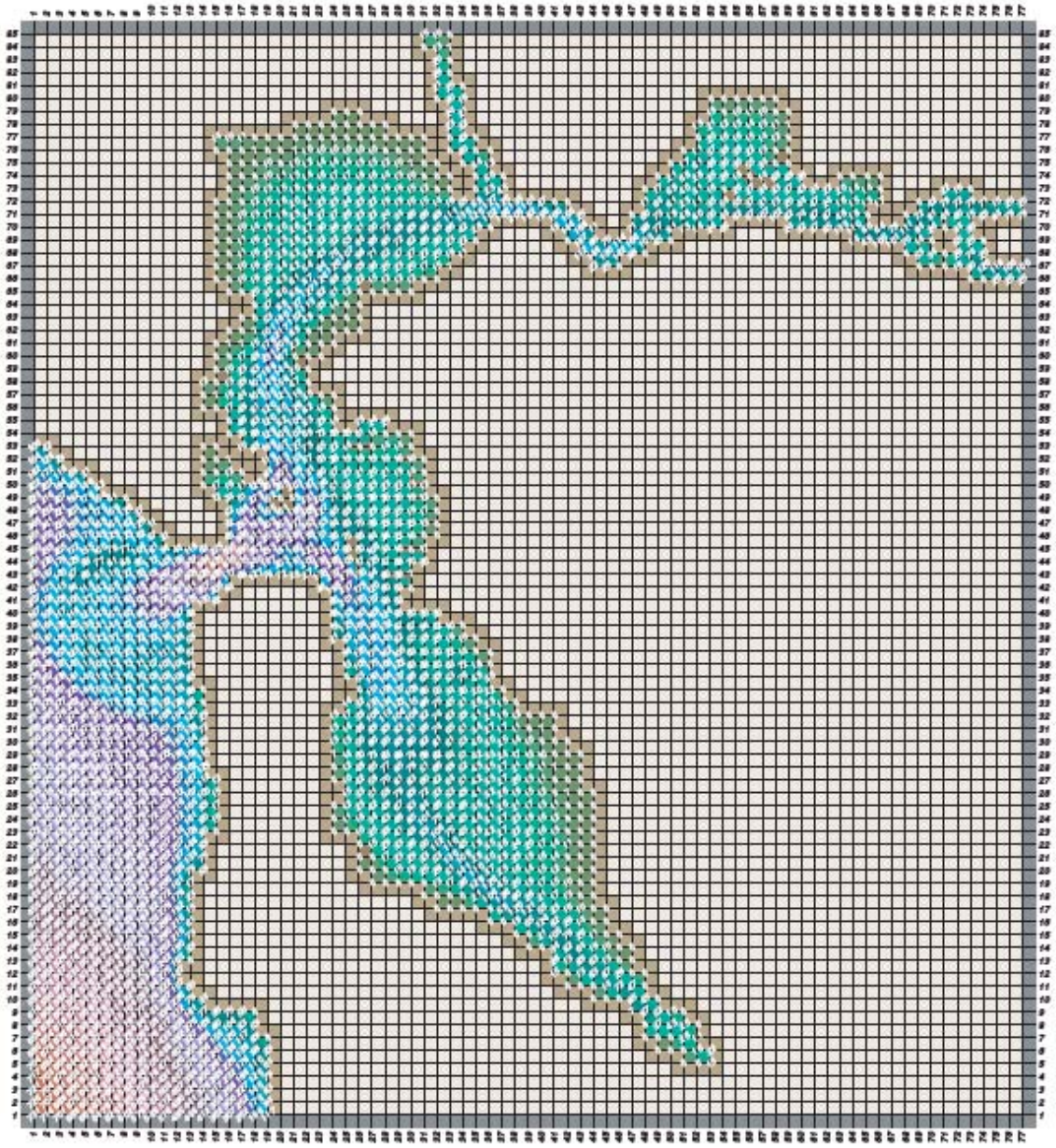

Figure 24. Grid, bathymetric data and computational domain of the San Francisco Bay and Estuary. It corresponds to a grid size of 1,000 m.

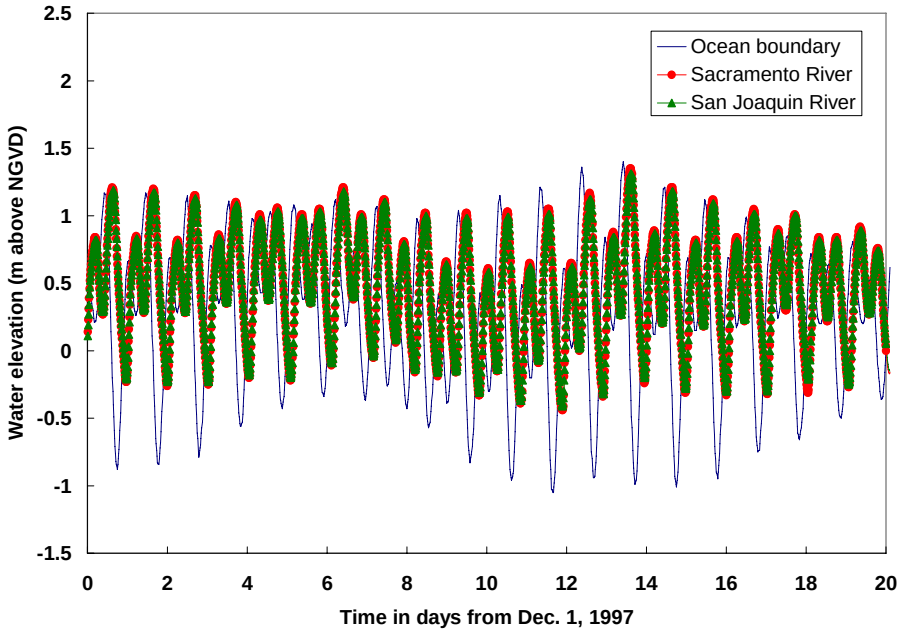

Figure 25. Boundary conditions at the ocean and in the Sacramento and San Joaquin Rivers for the scenario of December 1, 1997

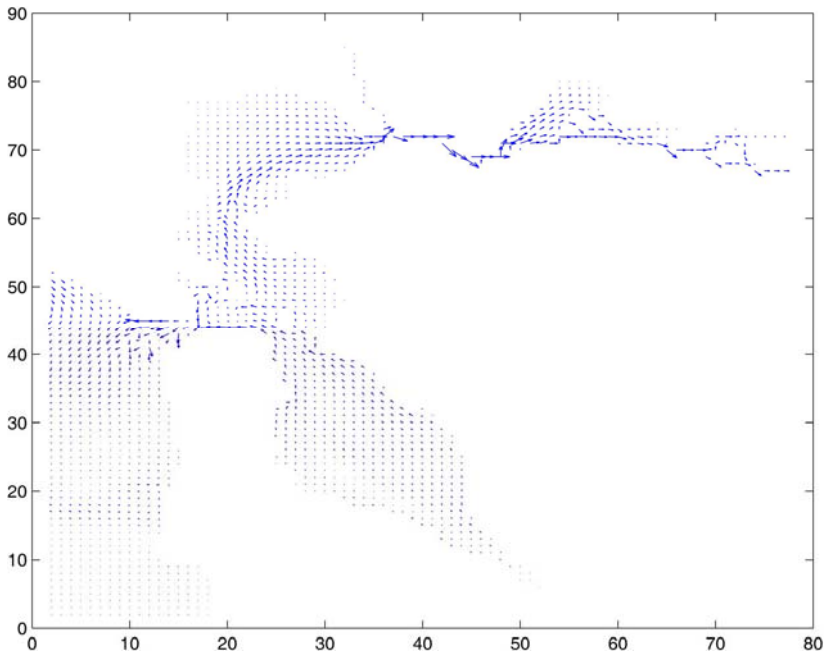

Figure 26. Velocity field at the free surface during a high weak tide in San Francisco Bay (hour 13)

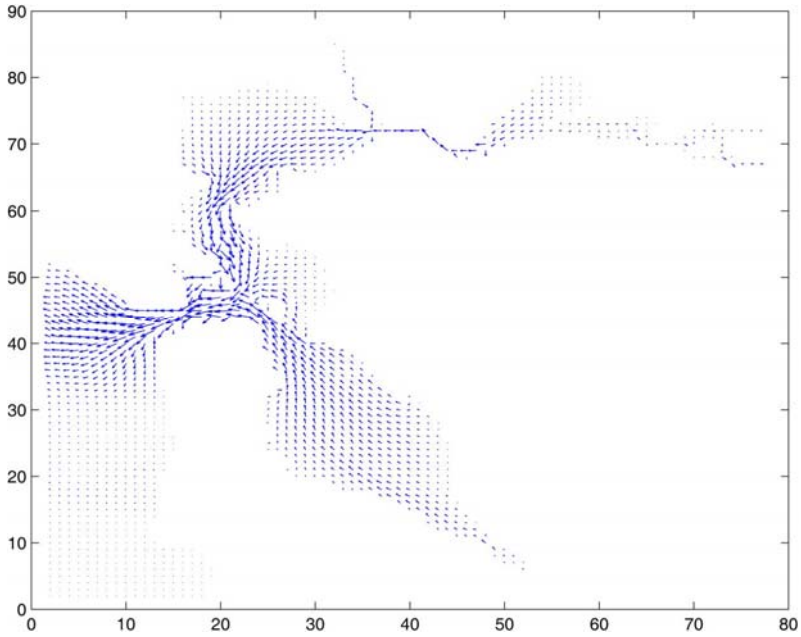

Figure 27. Velocity field at the free surface during an ebb tide in San Francisco Bay (hour 16)

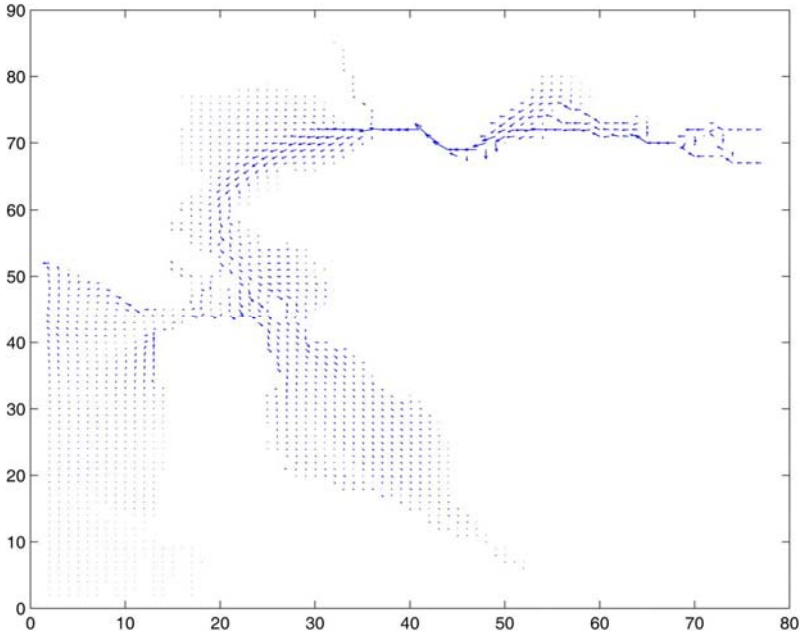

Figure 28. Velocity field at the free surface during a low weak tide in San Francisco Bay (hour 20)

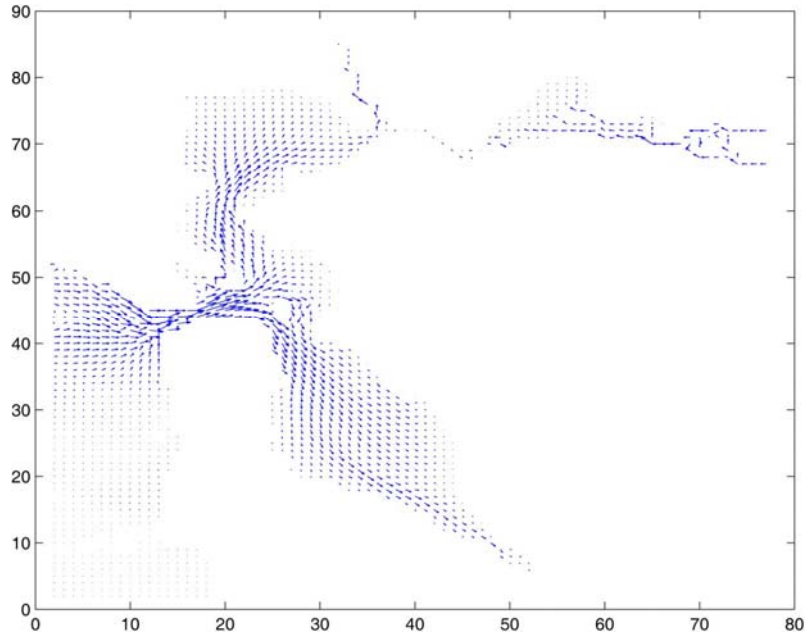

Figure 29. Velocity field at the free surface during a flood tide in San Francisco Bay (hour 23)

The Si3D program also writes time-series output data formatted for the USGS Velocity Profile Viewer written by John Donovan (see http://ca.water.usgs.gov/program/sfbay/vpv/). These data provide horizontal velocity vectors for each layer modeled at the nodes specified in the Si3D input file. For this test run, nodes (34, 71) and (15, 44) were specified according to the Si3D input file (Figures 30 and 31). These nodes correspond to the Carquinez Strait and the Golden Gate, respectively. The following two figures show velocity profiles for these two locations during the same time (hour 16). Other times can be found in:
http://cee.engr.ucdavis.edu/faculty/Bombardelli/bacteroidales.html

In these profiles, horizontal velocity is plotted for each vertical layer of the model. Water generally flows in the same direction at the Carquinez Strait and the Golden Gate during flooding and ebbing; however, water at these points will flow in opposing directions during weak tides. There is obviously a lag time between peaks of flow in the two stations, which is close to the square root of the product between the acceleration of gravity and the averaged water depth in the main channel in the San Pablo Bay. The Golden Gate is much deeper than the Carquinez Strait, and therefore, there are more vertical layers used to model flow at that location.

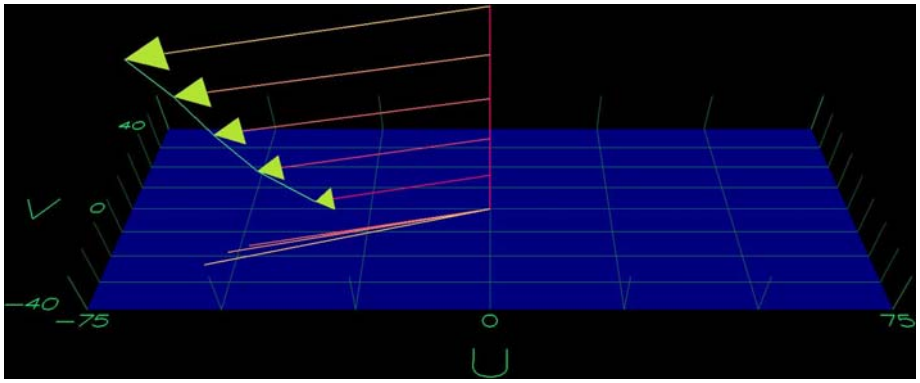

Figure 30. Velocity profile at the Carquinez Strait, node (34, 71), during an ebb tide in San Francisco Bay (hour 16)

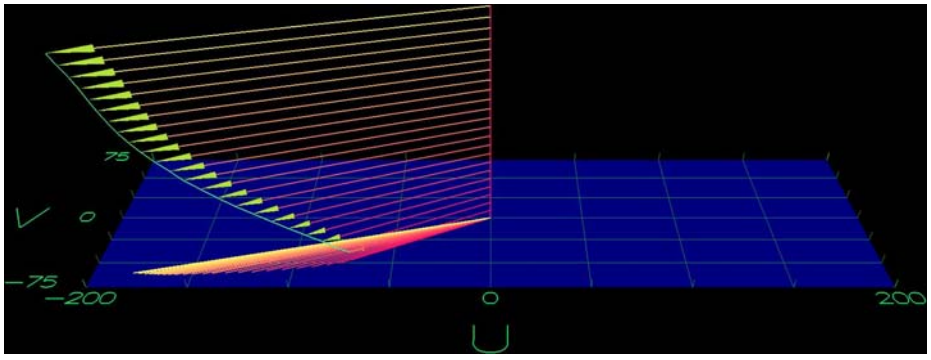

Figure 31. Velocity profile at the Golden Gate, node (15, 44), during an ebb tide in San Francisco Bay (hour 16)

We have also tested the response of the model to variations in mesh size in the vertical direction, to turbulence modeling, to the coefficient of flow resistance, and several numerical parameters.

Results for November 1 2007

Figure 32 shows the water stages at the ocean and inland boundaries, starting at 0 hs on October 20, 2007. These boundary conditions were input to the model to run this scenario, from October 20 to November 2, 2007. The ten days prior to the observation event (November 1, 2007) allow for a warm up of the model until the initial transitory stage disappears. Velocity fields in the entire domain were obtained every 8 hours. Time step was fixed in 300 seconds.

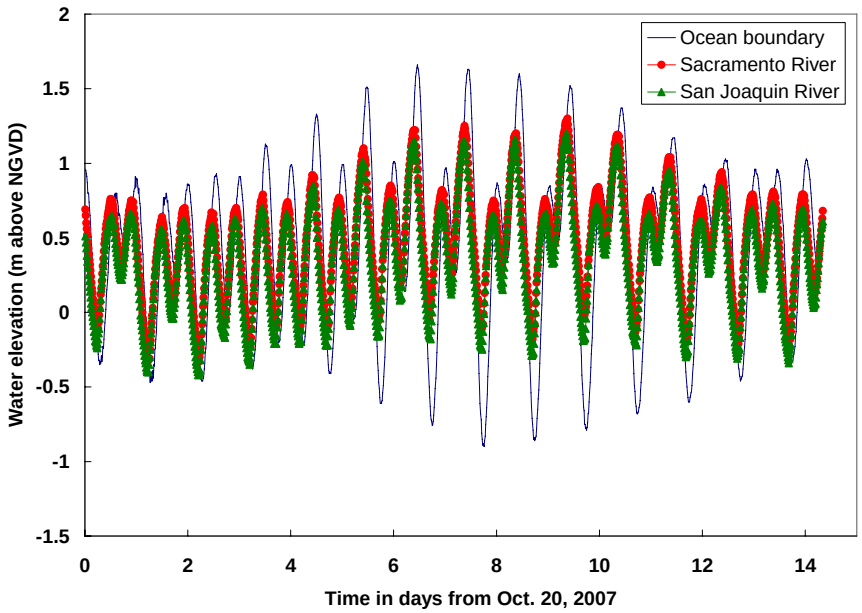

Figure 32. Boundary conditions at the ocean and in the Sacramento and San Joaquin Rivers for the scenario of November 1, 2007

Figures 33 to 36 show snapshots of the velocity vectors at the free surface for specific days in October and November. Similar patterns to those observed for December 1, 1997 are obtained. In particular, the flow conditions at 8 AM on November 1, 2007, when the field campaign started for that day and at 16 hs are shown, when the last station was visited.

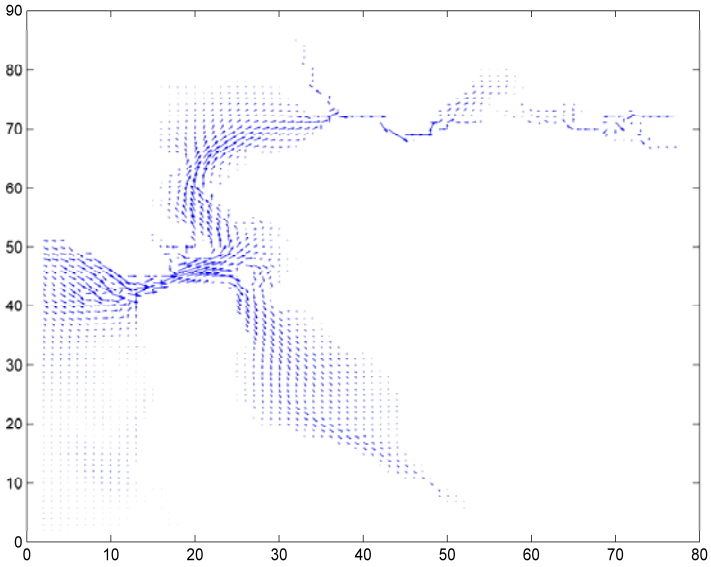

Figure 33. Velocity field at the free surface during a flood tide in San Francisco Bay at 16 hs on October 20, 2007

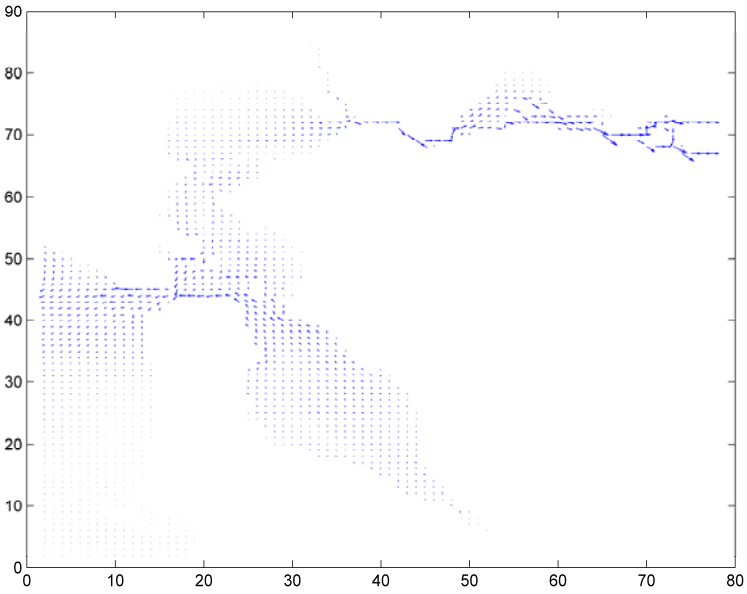

Figure 34. Velocity field at the free surface in San Francisco Bay at 0 hs on November 1, 2007

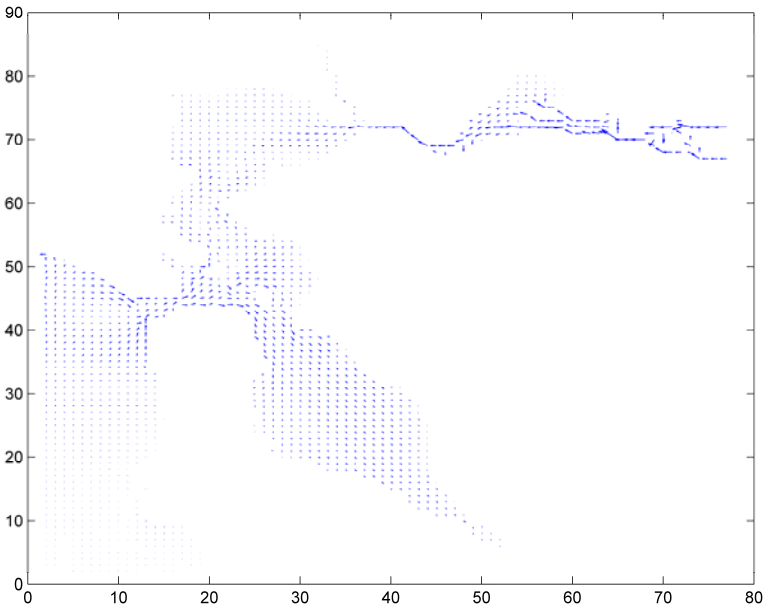

Figure 35. Velocity field at the free surface in San Francisco Bay at 8 hs on November 1, 2007

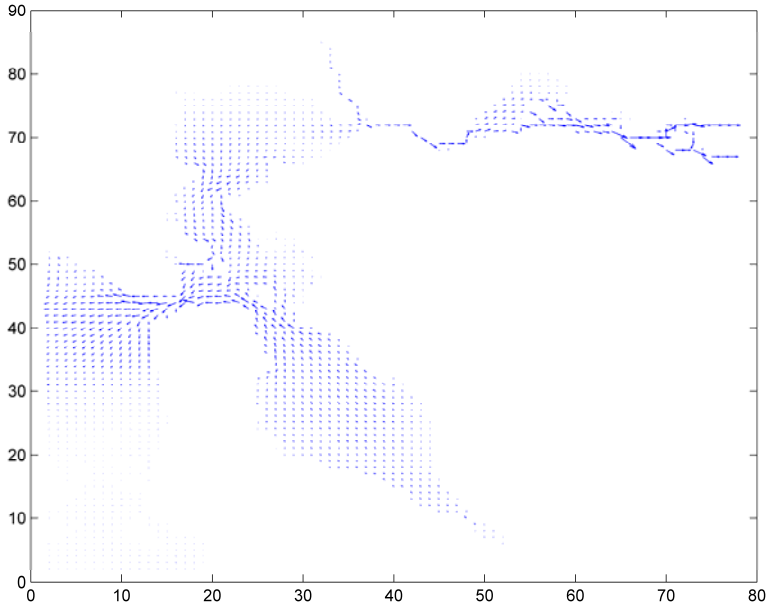

Figure 36. Velocity field at the free surface in San Francisco Bay at 16 hs on November 1, 2007

The numerical results also include time series at the stations of the field campaign. These time series were animated with the VPV program mentioned before, and the conditions at the sampling times were determined from them for model checking (see Section on comparison of model prediction with field data). Figure 37 shows a snapshot of the distribution of velocity vectors at the Sonoma Creek Island number 1, giving a velocity modulus of about 0.25 m/s. In this station, the water level varied from -1.11 to 2.05 m NGVD. Figures 38 and 39 show similar plots for Carquinez Strait and San Pablo Strait at the times of sampling. For the Carquinez Strait, water levels varied from -1.09 to 2.04 m NGVD.

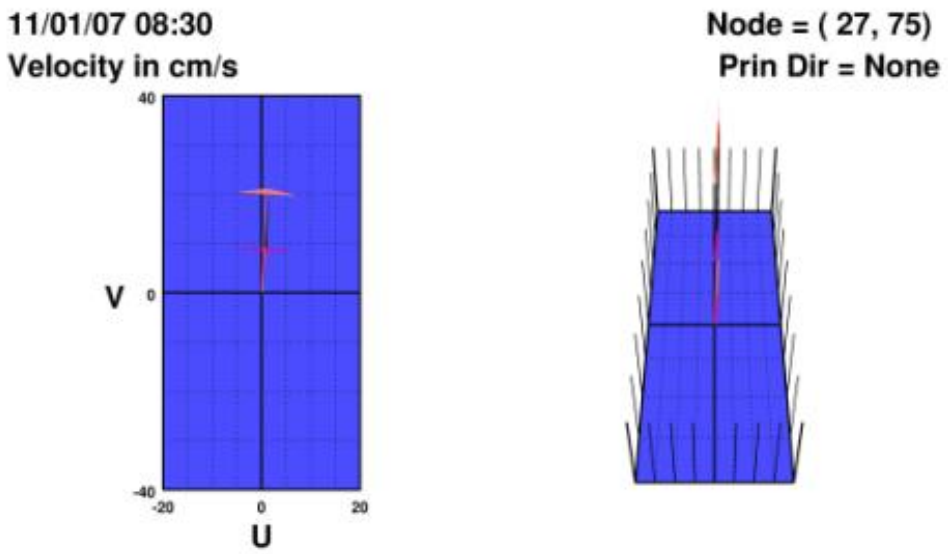

Figure 37. Snapshot of the vertical distribution of velocity vectors at the Sonoma Creek Island number 1 at the time of sampling

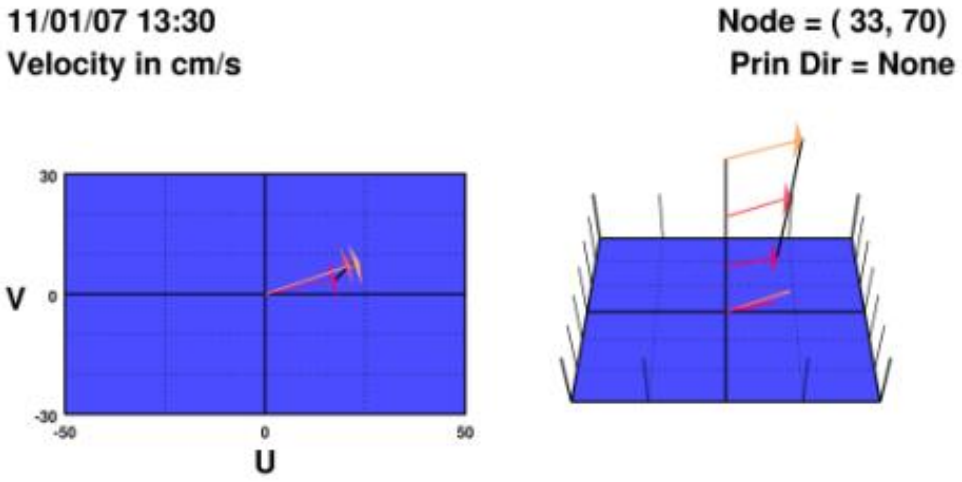

Figure 38. Snapshot of the vertical distribution of velocity vectors at the Carquinez Strait at the time of sampling

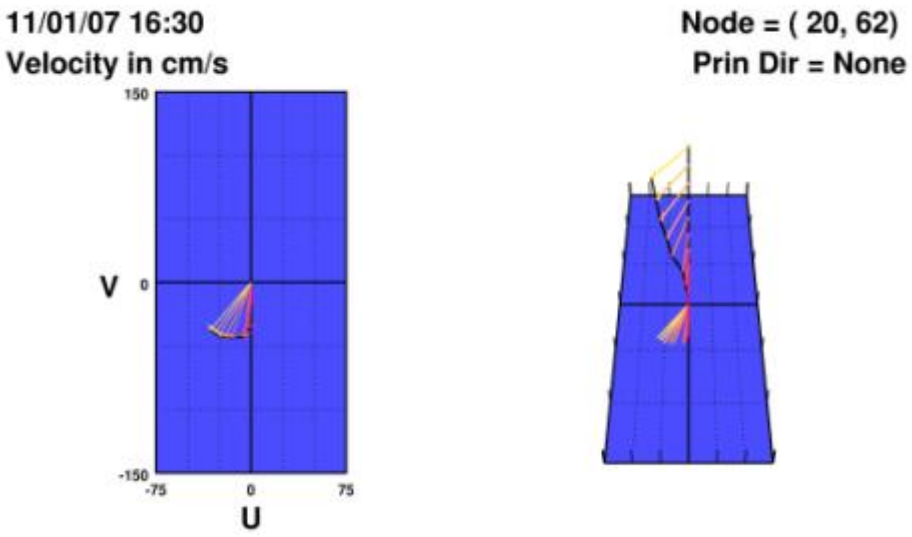

Figure 39. Snapshot of the vertical distribution of velocity vectors at the San Pablo Strait at the time of sampling

Results for January 15 2008

Figure 40 shows the water stages at the boundaries, starting at 0 hs on January 4, 2008. These boundary conditions were input to the model to run this scenario, from January 4 to January 16, 2008. Velocity fields in the entire domain were obtained every 8 hours. Note that the water levels in the rivers in the first six days are higher than those at the end of the period.

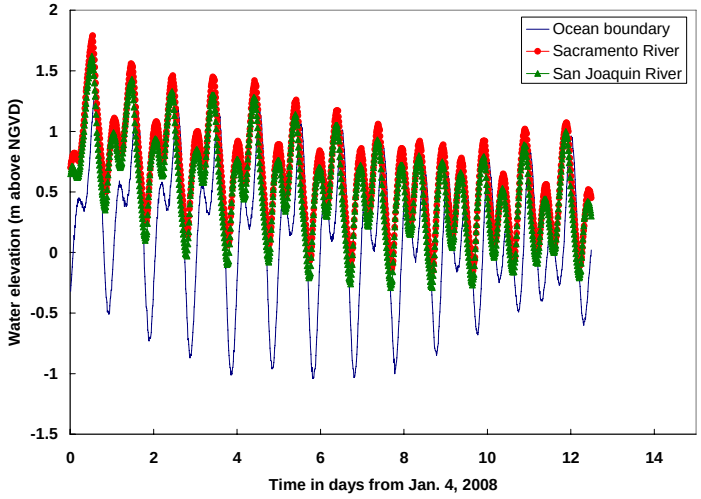

Figure 40. Boundary conditions at the ocean and in the Sacramento and San Joaquin Rivers for the scenario of January 15, 2008

Figures 41 to 43 show snapshots of the velocity vectors at the free surface for specific days in January, 2008.

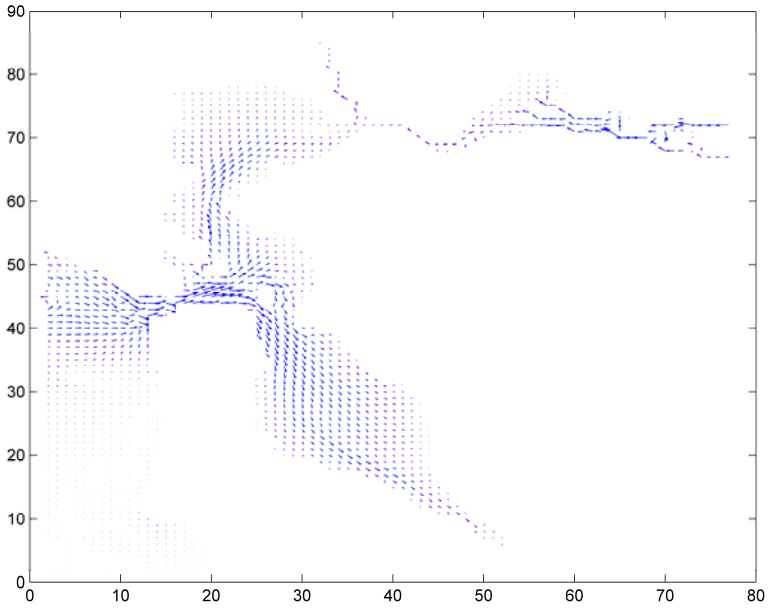

Figure 41. Velocity field at the free surface in San Francisco Bay at 16 hs on January 12, 2008

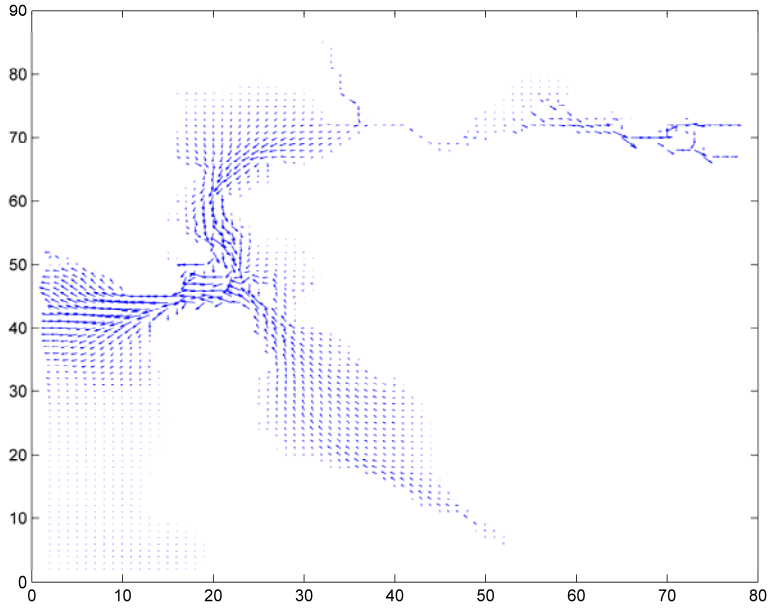

Figure 42. Velocity field at the free surface in San Francisco Bay at 0 hs on January 15, 2008

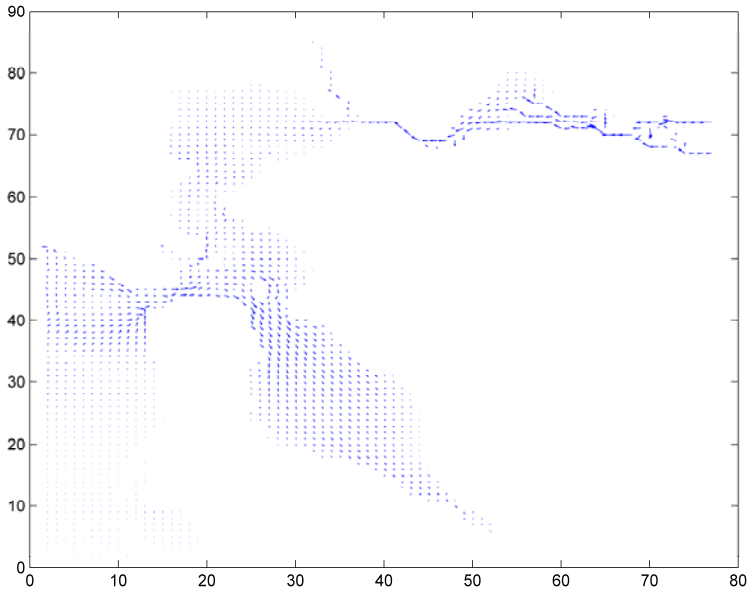

Figure 43. Velocity field at the free surface in San Francisco Bay at 16 hs on January 15, 2008

Processing data from field observations

The velocity data collected during the diverse field campaigns were analyzed using the software provided by the manufacturer. The observations were undertaken for no less than 10 minutes (in some cases for about 25 minutes) in each point selected (Figure 3). It is worth pointing out that velocity measurements of such frequency and duration are rare in studies associated with estuarine and river flows.

The instrument utilized is an ADCP (Acoustic Doppler Current Profiler). The working principle of the ADCP is based on the reflection of acoustic signals on moving particles in the flow. The three components of the velocity were observed in horizontal beams in the depth. During the measurements, the ADCP was attached to a boat.

Figure 44 shows one time series of the observations pertaining to March 5, 2008, at the Carquinez Strait Dillon Point, which lasted almost 15 minutes (please see top horizontal axis). The plot depicts the modulus of the velocity as a function of the bins on the right, counted from the free surface (at the top of the image), or expressed in meters on the left (the depth in the area was about 30 m). We can observe that the velocity magnitude at the top is of the order of 0.3 m/s. Figure 45 presents another time series obtained at the Napa River Mouth on May 25, 2008.

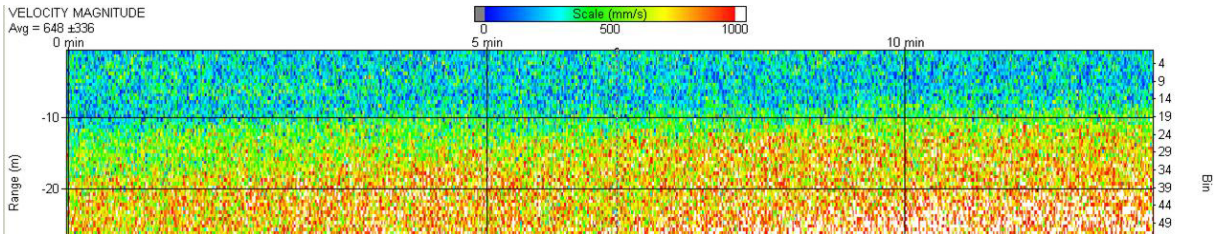

Figure 44. Time series of the velocity data pertaining to March 5, 2008, at the Carquinez Strait Dillon Point

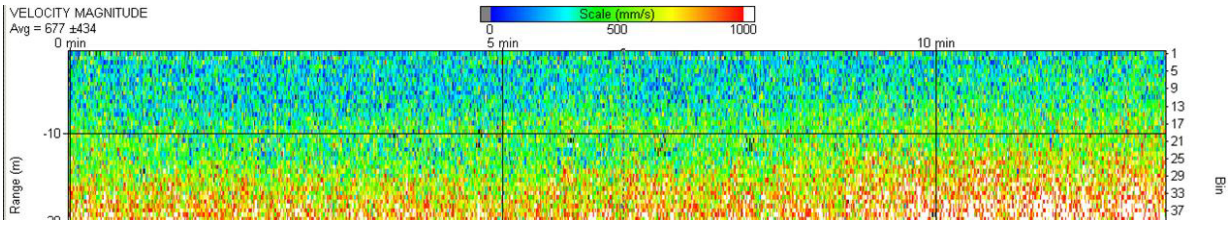

Figure 45. Time series of the velocity data obtained at the Napa River Mouth on May 25, 2008

The temporal series were averaged in time, obtaining vertical profiles of the three components of the velocity, and of the time average. Figure 46 shows a profile pertaining to the observations taken during March 5, 2008, in San Pablo Strait.

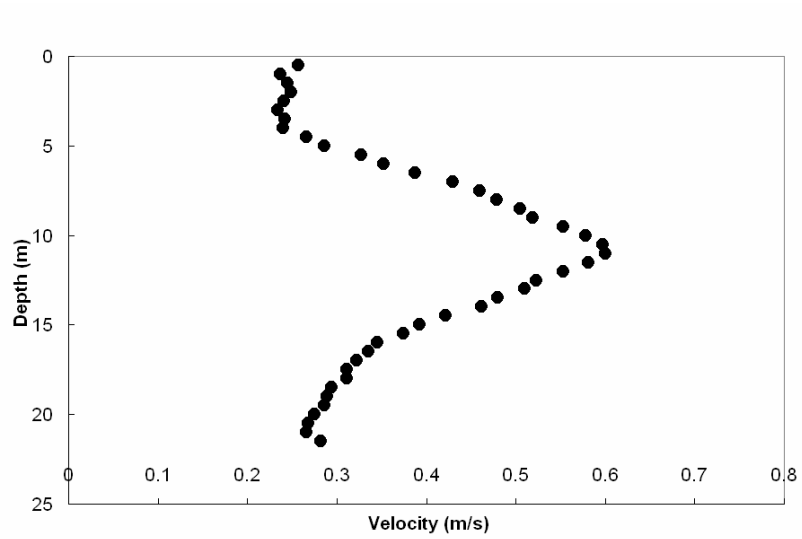

Figure 46. Vertical profile of velocity magnitude pertaining to the observations taken during March 5, 2008, in San Pablo Strait

Comparison of simulations with observations

The numerical results obtained with the Si3D code were compared with values of velocity observed during the field campaigns. The measured velocities were averaged in the measurement time to obtain representative values. A good agreement was observed, with differences on the order of 15% at most.

Discussion

In this study, a validated hollow fiber ultrafiltration method was combined with molecular DNA-based assays to quantify *Bacteroidales* genetic marker concentrations (universal, human-, cow-, and dog-specific) in environmental samples of San Pablo Bay during November 2007 to July 2008. Low levels of universal *Bacteroidales* genetic markers were found in all 6 monitoring campaigns at all sampling locations ranging from the entrance of freshwater sources to the bay, the outlet of the bay to the connecting San Francisco Bay, and inside the bay. *E. coli* and enterococci were present at low levels at a few sites, especially ones near freshwater sources. Environmental concentrations of universal *Bacteroidales* were quantified as gene copies per ml of water sample before filtration, and the relative ratios of human-specific to universal *Bacteroidales* were calculated for each sample to indicate human contribution to fecal contamination. Universal *Bacteroidales* markers were detected in all samples, indicating non host-specific fecal contamination. This 100% positive detection of *Bacteroidales* contrasted with only partial detection of *E. coli* and enterococci, suggesting that *Bacteroidales* may be a more suitable tracer of fecal pollution in this bay.

Human-specific *Bacteroidales* were detected in 75% of samples, while cow- and dog-specific *Bacteroidales* were found to be below detection limits in all but one (for dog) sample. It is possible that some fecal contamination of San Pablo Bay may have originated from other sources for which the appropriate host-specific assays have not yet been developed. During the study a newly available seagull-specific qPCR assay was validated and found to be broadly specific for seabirds. The assay could be applied in the future to archived environmental samples to estimate the contribution from sea birds to bacterial fecal loads in San Pablo Bay and its tributaries.

The human viruses (adeno- and enteroviruses) were not found at any locations during 6 sampling events. Taken together, the detection results of all assays indicated a low but persistent level of fecal contamination in San Pablo Bay, with seasonal increases in concentrations of *Bacteroidales* genetic markers as would be expected due to influence stormwater runoff.

The host-specific *Bacteroidales* assays have been used in other monitoring studies in California (Kildare et al., 2006; CREST, 2008) and even in a rural watershed of Kenya (Jenkins et al., submitted) and shown to have excellent predictive value for fecal

pollution sources. The concentrations of *Bacteroidales* genetic markers found in San Pablo Bay are generally much lower than those found in the arid region of Los Angeles River and those in the Calleguas Creek Watershed, both located in Southern California. Congruent with these observations, FIB counts were also generally low in San Pablo Bay.

Fate and transport models of fecal contamination in San Pablo Bay were developed, and they are in operative mode. Advective transport of *Bacteroidales*, a main mechanism, was modeled utilizing the Si3D model and hydrodynamic data that were available for San Pablo Bay, and compared (checked) with velocity data that were measured during the monitoring campaigns. The *Bacteroidales* concentrations can be computed with the Si3DWQ. The model developed in this study will help to (1) estimate the points of contaminant discharge based on locations and concentrations in the field; and (2) predict the concentrations in the bay both spatially and temporally. The model therefore prevents cost- and labor-intensive water monitoring of fecal contamination. Instead, it allows for the selection of fewer sampling locations that are needed to monitor the near-shore sites while the model is used to predict concentrations at other points inside the bay.

Conclusions

- Microbial source tracking using fecal *Bacteroidales* is an effective way to monitor fecal pollution of coastal waters. Low levels of the universal genetic marker are ubiquitous throughout San Pablo Bay. The human marker BacHum-UCD was found in 75% of all samples but no cow- and almost no dog-specific marker was detected.
- There was a poor correlation between *Bacteroidales* genetic markers and viable fecal indicator bacteria (FIB) due to the high number of nondetects for *E. coli* and enterococci. For the purpose of modeling the fate and transport of fecal inputs into San Pablo Bay (SPB), *Bacteroidales* are a more promising target than FIB.
- The Si3D model for SPB was used to pinpoint the best monitoring stations and field measurements of velocity profiles in the bay were successfully predicted with the code. The model is operational for the simulation of *Bacteroidales* genetic marker concentrations at different locations throughout the bay.
- No human viruses were detected in the study but the model can be applied to predict the concentration of any microbial target in the bay given a specific input concentration.
- In order to become accessible to intended end users the model interface needs to be further developed. In addition, sediment transport can play a major role in determining the fate of pathogens in coastal environments and the Si3D model would benefit from incorporating subroutines to describe such a mechanism.

List of publications

Bombardelli, F. A., and Jha, S. K. Hierarchical modeling of the dilute transport of suspended sediment in open channels. *Environmental Fluid Mechanics*. Published online.

McDonald, A.J. (2007) Advection-diffusion-reaction modeling of *Bacteroidales* in estuaries with a specific application to the San Pablo Bay. Master of Science Thesis. Department of Civil and Environmental Engineering, University of California, Davis.

Rajal, V.B., McSwain, B.S., Thompson, D.E., Leutenegger, C.M., Kildare, B. and Wuertz, S. (2007) Validation of hollow fiber ultrafiltration and real time PCR using bacteriophage PP7 as surrogate for the quantification of viruses from water samples, *Water Research,* 41:1411-1422.

Rajal, V.B., McSwain, B.S., Thompson, D.E., Leutenegger, C.M. and Wuertz, S. (2007) Molecular quantitative analysis of human viruses in California storm water, *Water Research*, 41:4287-4298.

Santo Domingo, J.W., Bambic, D.G., Edge, T.A. and Wuertz, S. (2007) Quo vadis source tracking? Towards a strategic framework for environmental monitoring of fecal pollution, *Water Research,* 41: 3539-3552.

References

Bernhard, A.E. and Field, K.G. (2000) A PCR assay to discriminate human and ruminant feces on the basis of host differences in *Bacteroides-Prevotella* genes encoding 16S rRNA, *Applied and Environmental Microbiology,* 66(10): 4571-4574.

California Regional Water Quality Control Board, San Francisco Bay Region (CRWQCB) 2007. San Francisco Bay Basin (Region 2) Water Quality Control Plan (Basin Plan). Chapter 3: Water Quality Objectives.

Cleaner Rivers through Effective Stakeholder-led TMDLs (CREST) (2008) Los Angeles river bacteria source identification study final report, November 2008. http://www.crestmdl.org/studies/bsi_final_docs.html

Dick, L.K. and Field, K.G. (2004) Rapid estimation of numbers of fecal *Bacteroidetes* by use of a quantitative PCR assay for 16S rRNA genes, *Applied and Environmental Microbiology,* 70(9): 5695-5697.

Dick, L.K., Bernhard, A.E., Brodeur, T.J., Santo Domingo, J.W., Simpson, J.M., Walters, S.P., and Field, K.G. (2005) Host distributions of uncultivated fecal *Bacteroidales* bacteria reveal genetic markers for fecal source identification, *Applied and Environmental Microbiology,* 71: 33184-3191.

Eaton, A.L., Clersceri, L.S., Rice, E.W., Greenberg, A.E. (2005) Standard methods for the examination of water and wastewater, 21st ed. American Public Health Association (APHA),
American Water Works Association (AWWA), Water Environment Federation (WEF).

Fogarty, L.R. and Voytek, M.A. (2005) Comparison of *Bacteroides-Prevotella* 16S rRNA genetic markers for fecal samples from different animal species, *Applied and Environmental Microbiology,* 71(10): 5999-6007.

Gersberg, R.M., Matkovits, M., Dodge, D., McPherson, T., and Boland, J.M. (1995) Experimental opening of a coastal California lagoon: Effect on bacteriological quality of recreational ocean waters, *Journal of Environmental Health,* 58: 24-29.

Jiang, S.C., and Chu, W. (2004) PCR detection of pathogenic viruses in southern California urban rivers, *Journal of Applied Microbiology,* 97: 17-28.

Jenkins, M.W., Tiwari, S, Lorente, M., Maina-Gichaba, C., and Wuertz, S. Identifying human and livestock sources of fecal contamination in Kenya with host-specific *Bacteroidales* assays developed in the United States and Europe. Submitted for publication

Kildare, B., Rajal, V., Tiwari, S., Thompson, D., McSwain, B., Bambic, D.,Reide, G. and Wuertz, S. (2006) Calleguas Creek watershed quantitative microbial source tracking study. Report to Calleguas Creek Stakeholders, prepared by UC Davis in Cooperation with Larry Walker Associates, April 2006.

Kildare, B.J., Leutenegger, C.M., McSwain, B.S., Bambic, D., Rajal, V.B. and Wuertz S. (2007) 16S rRNA-based assays for quantitative detection of niversal, human-, cow-, and dog-specific fecal *Bacteroidales*: A Bayesian approach, *Water Research* 41:3701-3715.

Layton, A., McKay, L., Williams, D., Garrett, V., Gentry, R. and Saylor, G. (2006) Development of *Bacteroides* 16S rRNA gene Taqman-based real-time PCR assays for estimation of total, human, and bovine fecal pollution in water, *Applied and Environmental Microbiology,* 72:4214-4224.

Lu, J., Santo Domingo, J. W., Lamendella, R., Edge, T. and Hill, S. (2008) Phylogenetic diversity and molecular detection of bacteria in gull feces, *Applied and Environmental Microbiology,* 74, 3969-3976.

McDonald, A.J. (2007) Advection-diffusion-reaction modeling of *Bacteroidales* in estuaries with a specific application to the San Pablo Bay. Master of Science Thesis. Department of Civil and Environmental Engineering, University of California, Davis.

Okabe, S., Okayama, N., Savichtcheva, O. and Ito, T (2007) Quantification of host-specific *Bacteroides-Prevotella* 16S rRNA genetic markers for assessment of fecal pollution in freshwater, *Applied Microbiology and Biotechnology,* 74(4), 890-901.

Rajal, V., Thompson, D., Kildare, B., Tiwari, S., McSwain, B., and Wuertz, S. (2005) Management of pathogens associated with storm water discharge: methodology for quantitative molecular determination of viruses, bacteria, and protozoa. Interim Report Prepared for the Environmental Division of California Department of Transportation, Task Order no. 19.

Rajal, V., McSwain, B., Thompson, D., Leutenegger, C., Kildare, B., and Wuertz, S. (2007a) Validation of hollow fiber ultrafiltration and real-time PCR using bacteriophage PP7 as surrogate for the quantification of viruses from water samples, *Water Research,* 41(7), 1411-1422.

Rajal, V. B., McSwain, B.S., Thompson, D.E., Leutenegger, C.M. and Wuertz, S. (2007b) Molecular quantitative analysis of human viruses in California storm water, *Water Research,* 41(7),4287-4298.

Rayl, A.J.S. (2001) Human viruses at sea, *Scientist,* 15: 19-19.

Reischer, G.H., Kasper, D.C., Steinborn, R., Mach, R.L. and Farnleitner, A.H. (2006) Quantitative PCR method for sensitive detection of ruminant fecal pollution in freshwater and evaluation of this method in alpine karstic regions, *Applied and Environmental Microbiology*, 72(8), 5610-5614.

Reischer, G.H., Kasper, D.C., Steinborn, R., Farnleitner, A.H. and Mach, R.L. (2007) A quantitative real-time PCR assay for the highly sensitive and specific detection of human faecal influence in spring water from a large alpine catchment area, *Letters in Applied Microbiology*, 44(4), 351-356.

Rose, J.B. (2000) Human viruses in the coastal waters of Florida, *Coastlines*, pp. 7-8.

Savichtcheva, O., Okayama, N. and Okabe, S. (2007) Relationships between *Bacteroides* 16S rRNA genetic markers and presence of bacterial enteric pathogens and conventional fecal indicators, *Water Research*, 41(16):3615-28.

Seurinck, S., Defoirdt, T., Verstraete, W. and Siciliano, S.D. (2005) Detection and quantification of the human-specific HF183 *Bacteroides* 16S rRNA genetic marker with real-time PCR for assessment of human faecal pollution in freshwater, *Environmental Microbiology*, 7(2), 249-259.

Smith, P. E. (1997). A three-dimensional, finite-difference model for estuarine circulation. Ph.D. Dissertation, Department of Civil and Environmental Engineering, UC Davis.

Smith, P. E., and Larock, B. E. (1997) Semi-implicit numerical schemes for 3-D flow modeling, *Proc. 27th IAHR Congress*, San Francisco, CA.

Smith, J.E., and Perdek, J.M. (2004) Assessment and management of watershed microbial contaminants. *Critical Reviews in Environmental Science and Technology*, 34: 109-139.

Straub, T.M., and Chandler, D.P. (2003) Towards a unified system for detecting waterborne pathogens, *Journal of Microbiological Methods,* 53: 185-197.

U.S. EPA (2007a). Criteria development plan & schedule—recreational water quality criteria: U.S. EPA Offices of Water and Research and Development: Washington, D.C., United States.

U.S. EPA (2007b). Critical path science plan for the development of new or revised recreational water quality criteria, U.S. EPA Office of Research and Development: Washington, D.C., United States.

Walters, S.P., Gannon, V.P.J. and Field, K.G. (2007) Detection of *Bacteroidales* fecal indicators and the zoonotic pathogens *E. coli* O157 : H7, *Salmonella*, and *Campylobacter* in river water, *Environmental Science & Technology,* 41(6), 1856-1862.